https://dx.doi.org/10.1016/j.tre.2021.102555

Optimization of Multi-type Traffic Sensor Locations for Estimation of Multi-period Origin-Destination Demands with Covariance Effects

Hao Fu[a,*], William H.K. Lam[a], Hu Shao[b], Lina Kattan[c], Mostafa Salari[c]

[a] Department of Civil and Environmental Engineering, The Hong Kong Polytechnic University, Hung Hom, Kowloon, Hong Kong, China

[b] School of Mathematics, China University of Mining and Technology, Xuzhou, Jiangsu 221116, China

[c] Department of Civil and Environmental Engineering, Schulich School of Engineering, University of Calgary, Calgary, Alberta, Canada

* Corresponding author, E-mail address: hao.fu@connect.polyu.hk

Abstract

The hourly traffic flows between various origin-destination (OD) pairs fluctuate by time of day and day of the year. These multi-period OD demands are statistically correlated with one another because of the inter-relationships of travel patterns over time. In this paper, with a focus on the covariance relationship of OD demands in multiple periods, a novel model is proposed for optimizing the allocations of multi-type traffic sensors by minimizing the uncertainty of OD demand estimates. In the proposed model, both the number and locations of multi-type traffic sensors, including point sensors and automatic vehicle identification (AVI) sensors, are optimized simultaneously with consideration of budget and associated constraints. The mathematical properties of the proposed model are studied to show the significance of multi-period OD flow covariance in the sensor location problem and to examine the trade-off between point sensors and AVI sensors. The firefly algorithm is adapted to solve the problem of multi-type traffic sensor locations for multi-period OD demand estimation. To enhance the estimation efficiency, a Kalman filter method based on the principal component analysis is adopted to extract the essential features of the OD demands and then estimate multi-period OD demand. Numerical examples are presented to demonstrate the effects of OD demand covariance in multiple periods for the multi-type sensor allocation problem.

Keywords: Sensor location problem, Multi-type traffic sensors, Multi-period OD demand estimation, Statistical covariance

1 Introduction

The origin-destination (OD) vehicular flow is one of the most important inputs for transportation management and traffic control (Caggiani et al., 2013). The hourly OD demand is stochastic and fluctuates by time of day and day of the year due to recurrent and non-recurrent traffic conditions in road networks (Huang, 2002). For estimation of stochastic hourly OD demand, an efficient and economical way is based on vehicular flows, which in turn depends on the number, type, and locations of traffic sensors.

The majority of the sensor location problems (SLP), namely the identification of number and locations of traffic sensors, focus on one sensor type particularly to estimate peak period mean OD demand. However, multi-period stochastic traffic flows, including both mean and covariance play an increasingly

significant role to gain more insights into various travel patterns over time. Multiple types of sensors have emerged and can be integrated with the advancement in sensing and communication technologies. The problem becomes much more complicated when locating multi-type sensors at the same time and for multi-period OD estimation because of the inherent nature of SLP and OD demand estimation. This paper takes further steps in this direction to propose a more generalized model by optimizing multi-type traffic sensor location for OD demand estimation with explicit consideration of two significant features of OD demand:

- statistical characteristics, including spatial, temporal, and multi-period covariance of hourly OD flows;
- variation of traffic flows by time of day and day of the year.

The proposed model in this paper is capable of optimizing different types of traffic sensors at the same time for multi-period OD demand estimation including its mean and covariance. The inter-relationships between OD demands in different time periods and between different sensor types are intensively studied from both mathematical and numerical aspects.

1.1 Covariance of OD demand in multiple periods

The traffic demands exhibit time-to-time and day-to-day variability due to hourly, daily, and seasonal travel patterns in a road network (Shao et al., 2014; Meng et al., 2015a). Furthermore, the traffic flows of various OD pairs in multiple periods are highly correlated with one another because of the phenomenon of joint travel behavior and the inter-relationships of travel patterns in different periods (Ballis and Dimitriou, 2020). Elucidating these patterns of traffic flow for multiple periods can significantly benefit transportation planning and management.

The OD demands in multiple periods show spatial, temporal, and multi-period covariance in road networks. Specifically, as depicted in Shao et al. (2014), the covariance of OD flows in a spatial manner represents the statistical correlation of traffic flows within the same time period (e.g., morning peak period) among various OD pairs. Temporal covariance of OD flows represents the correlation of vehicular flow for the same OD pair but among different time periods (i.e., 8:00 –9:00 and 17:00–18:00). In addition to spatial and temporal covariance, OD demands may also show multi-period covariance, i.e., correlation of OD demands for different OD pairs over different time periods. In fact, these three types of OD demand covariances simultaneously contribute to the stochasticity of OD demands in multiple periods.

In stochastic transportation networks, the covariance of OD demands in multiple periods is often overlooked in the OD demand estimation problem. Using the mean of OD demand estimates without consideration of variance and covariance may lead to biased outputs as the variation of travel patterns over time cannot be adequately captured (Fu et al., 2019). In the last decade, a few studies have made important contributions in showing the importance of capturing OD trip chaining behavior and temporal interaction. For instance, to explicitly consider the trip chaining behavior, Cantelmo et al. (2020) developed a new state-space framework based on a Kalman filter for OD demand estimation. Djukic et al. (2012) and Krishnakumari et al. (2020) considered the variation of OD demand by time of day and day of the year using a principal component analysis (PCA) method to reduce the dimensionality of high-dimensional OD matrices. A quasi-dynamic extended Kalman filter was developed by Marzano et al.

(2018) to estimate stochastic OD demand more efficiently. Recently, several studies have focused on estimating the covariance relationship of OD demand rather than the mean OD demand (Shao et al., 2014, 2015).

Clearly, the above studies have demonstrated that the covariance of OD demands plays an essential feature in stochastic OD demand estimation problems. However, less attention has been paid to the estimation of OD demand while considering the spatial, temporal, and multi-period covariances simultaneously. Such consideration is a significant input for transportation planning and management and thus a vital extension of the current studies to formulate the stochastic OD demand estimation considering different OD demand covariances.

1.2 Sensor location problems for OD demand estimation

In practice, the locations of traffic sensors can be determined for many purposes, such as (a) to estimate traffic flows on links and/or paths (Castillo et al., 2011; Gentili and Mirchandani, 2012), (b) to estimate OD demand (Zhou and List, 2010; Simonelli et al., 2012; Fu et al., 2019), (c) to observe the exact flows on links or paths (Fu et al., 2016; Xu et al., 2016; Salari et al., 2019), and (d) to estimate link or path travel times (Xing et al., 2013; Park and Haghani, 2015; Gentili and Mirchandani, 2018). Among these different purposes of sensor installation, the OD estimation problem, in general, is of importance for the operation and planning of transportation systems, especially to provide a solid base of traffic control and route guidance schemes. In view of this, the research effort of this paper is directed toward the sensor location problem for OD demand estimation.

From traffic planners' aspects, traffic demands that can be inferred from traffic counts are intrinsically fundamental traffic characteristics. However, OD demand estimation is usually an underdetermined problem because the number of traffic sensors is often much smaller than the number of unknown OD pairs, especially in a large-scale road network. Many studies have proposed various models to deal with this underdetermined system, and thus confine the search space around meaningful solutions. For example, utilizing prior OD demand information obtained from surveys or simulation models as part of the model formulation incorporates important structural information related to the temporal and spatial distribution of trip making activities. On the basis of the observations from traffic sensors, an entropy maximization model was first developed by Van Zuylen and Willumsen (1980) to find the most likely OD demand matrix. Maher (1983) proposed analytical models to update the prior mean and variance of static OD demand using Bayesian theory.

In fact, the number, type, and locations of sensors significantly affect the quality of the OD demand estimates. Most researchers have elected to optimize traffic sensor locations with respect to the accuracy of mean OD demand estimation (Bianco et al., 2001; Xiong et al., 2014). Several recent studies of the SLP have focused on the variances of OD flow to minimize the error of OD demand estimates considering the daily variation of travel patterns (Zhou and List, 2010; Simonelli et al., 2012). In Fu et al. (2019), we further examined the significance of spatial covariance of OD demand during peak hour periods on SLP.

However, only the OD demands in one specific time span, e.g., the morning peak, were considered in these studies such that only the spatial information can be incorporated. As both spatial and temporal information about OD demands can intrinsically facilitate routing policies, transportation management,

and traffic control for various periods, estimation of multi-period OD demands has assumed growing importance in the context of intelligent transportation systems (Meng and Wang, 2011; Ohazulike et al., 2013; Meng et al., 2015b). Hence, there is an urgent need to generalize the traffic sensor location method for multi-period OD demand estimation with a particular emphasis on spatial, temporal, and multi-period covariances.

In the literature, there are many indexes to measure the model performance for sensor location and OD demand estimation problems. For instance, some prominent statistical measurements including mean absolute error, mean absolute percentage error, mean square error, root mean square error, and so forth have been widely used (Cascetta, 2009; Hu et al., 2016). However, the true values of OD demand, which are necessary for these measurements, can hardly be obtained in practice.

Apart from these statistical measurements, some scholars have proposed other criteria to evaluate the performance of estimated OD demand without the true values. Yang et al. (1991) proposed a maximum possible relative error to measure the maximum deviation of estimated OD demand from true values. Bierlaire (2002) proposed a total demand scale to calculate the difference between the maximum and minimum possible total OD demand estimates constrained by sensor measurements. Chootinan and Chen (2011) further developed a general demand scale to assess the accuracy of OD demand estimates from traffic sensors. Zhou and List (2010) and Xing et al. (2013) proposed the percentage of reduction in variance to measure the quality of sensor locations for OD demand estimation and travel time estimation, respectively.

1.3 Notes on the types of traffic sensors

In the transportation monitoring system, various types of traffic sensors are installed in road networks to monitor traffic conditions, and especially to help coordinate emergency responses to major collisions, extreme weather conditions, and abnormal incidents (Zhu et al., 2014; Siripirote et al., 2020).

The two main categories of traffic sensors are point sensors and automatic vehicle identification (AVI) sensors (Fu et al., 2017). Point sensors detect the entire flow passing through a location installed with the sensor. For instance, inductive-loop vehicle detectors can detect all vehicles passing a certain point using a moving magnet to induce an electric current in a nearby wire. AVI sensors, also referred to as point-to-point sensors in the literature, can basically record vehicle location, identification, and time stamp. According to Antoniou et al. (2004), AVI sensors can be classified into three groups: (i) area-wide tracking sensors (e.g., Global Positioning Systems and cell phone tracking systems), (ii) location-based entire vehicle identification sensors (e.g., automatic license plate recognition detectors), and (iii) location-based partial vehicle identification sensors (e.g., radio-frequency identification readers, Bluetooth detectors, and Wi-Fi systems). Sensors in Group (i) can track vehicles throughout the entire road network. Sensors in Group (ii) can identify all vehicles in a short-range area, as all vehicles should, by law, have a license plate in a visible position. Sensors in Group (iii) can recognize only a portion of vehicles equipped with specific tags in a short-range area. The AVI sensors considered in this paper belong to Group (iii) which are location-based partial vehicle identification sensors. These AVI sensors normally have two main functions: counting the number of tagged vehicles passing a specific sensor location, and matching the tagged vehicles at different locations for recording partial path flows.

The traffic data provided by various traffic sensor types can be integrated for multi-period OD demand estimation. To take full advantage of the presence of point sensors and emerging AVI sensors in a road network, many researchers have proposed various models to incorporate the data obtained from both sensor types for OD estimation (Antoniou et al., 2004; Hu et al., 2016). For instance, Antoniou et al. (2004) developed a new methodology for the incorporation of AVI data into OD estimation and prediction to improve estimation accuracy. Hu et al. (2016) proposed an integrated two-stage model to address the heterogeneous sensor location problem and OD demand estimation, where the error of the OD demand estimates occurring from the second-stage model is regarded as the feedback to modify the sensor location schemes.

Although some recent studies have tried to integrate the data from multi-type sensors, where these sensors should be installed in a road network and particularly how they should cooperate with each other at the planning stage, have not been intensively examined. To fill this gap, this paper proposes a new model to coordinately install multi-type traffic sensors including AVI sensors and point sensors for more accurate multi-period OD demand estimation, by exploiting the spatial, temporal, and multi-period covariance information of traffic flow.

1.4 Motivations and contributions

1.4.1 Motivating example

As mentioned above, covariance effects of hourly OD demand in multiple periods can result from different factors, such as hourly and daily variation of travel patterns, change of network topology, and joint travel behavior. For an intuitive explanation, the illustrative example related to joint travel behavior is presented to demonstrate the existence of OD demand covariance in multiple periods.

Joint travel behavior refers to how people consider the travel behaviors/choices of other household members or persons in their social networks when making their own travel choices (Bhat et al., 2013). Household members often need to decide how to share jointly owned vehicle(s) to conduct their daily activities. In this paper, joint travel behaviors include more than one trip with at least two household members (Cascetta, 2009). More specifically, if a joint travel behavior is conducted, there should be at least two different OD pairs.

An example is presented in this subsection to intuitively illustrate the relationship between joint travel behavior and OD demand, and to manifest the significance of spatial, temporal, and multi-period covariance. As shown in Fig. 1, the example network consists of six OD pairs {(3,2), (2,6), (3,6), (2,3), (6,2), (6,3)} with Node 2, Node 3, and Node 6 respectively representing the school, home, and office. The weekday morning peak hour and evening peak hour are represented by h_1 and h_2, respectively. For convenience, six OD pairs in the illustrative network are numbered from 1 to 6 with OD(1) = (3,2), OD(2) = (2,6), OD(3) = (3,6), OD(4) = (2,3), OD(5) = (6,2) and OD(6) = (6,3). $q_{w(h_x)}$ ($w = 1, \dots, 6$ and $x = 1,2$) represents traffic demand of OD pair *w* in time period h_x. $\sigma_{1(h_1),2(h_1)}$ stands for the OD demand covariance between OD pairs 1 and 2 in time period h_1. Similarly, $\sigma_{2(h_1),6(h_2)}$ stands for the OD demand covariance between OD pair 2 in time period h_1 and OD pair 6 in time period h_2.

Consider a joint travel behavior conducted by a spouse and a child as an example. Specifically, in the weekday morning peak hour (h_1), a spouse will drive the child to school first (i.e., OD pair (3, 2)) and

then drive to the office alone to work (i.e., OD pair (2, 6)). As such, two OD demands (i.e., one is from Node 3 to Node 2, and another is from Node 2 to Node 6) will be generated by such joint travel behavior in the weekday morning peak hour (h_1). In the weekday evening peak hour (h_2), the spouse has two options: (i) go back home directly (i.e., OD pair (6, 3)) while his/her child could take public transport or a school bus to go back home, or (ii) go to school to pick up his/her child (i.e., OD pair (6, 2)), then back home together (i.e., OD pair (2, 3)). Option (i) generates only one OD demand traveling from node 6 to node 3 directly, while option (ii), a joint travel behavior, splits the original demand into two OD demands (i.e., one is from Node 6 to Node 2, and another is from Node 2 to Node 3) and is similar to that in the morning peak hour.

Under such circumstances, a spatial covariance relationship exists between OD pairs (3,2) and (2,6) in the morning peak hour (i.e., $\sigma_{1(h_1),2(h_1)}$) due to the joint travel behavior by the spouse and the child. On the one hand, in the evening peak hour, if the spouse chooses option (i), the covariance relationship between OD pair (2,6) in the morning peak hour and OD pair (6,3) in the evening peak hour denoted as $\sigma_{2(h_1),6(h_2)}$ will be outstanding. On the other hand, if the spouse chooses option (ii), the covariances among OD pair (2,6) in the morning peak hour, OD pair (6,2), and OD pair (2,3) in the evening peak hour will be large.

Note that the joint travel behavior can be reflected by the vehicle occupancy data reported from "The Annual Traffic Census 2017" of Hong Kong (Transport Department, 2018). Vehicle occupancy is the number of persons in a vehicle including both driver and passengers. It has been pointed out in the literature that joint travel behaviors (including both carpooling and ridesharing for travel with or without the same OD pair) would lead to a larger vehicle occupancy (Goel et al., 2016; Yin et al., 2017). For instance, Goel et al. (2016) mentioned that vehicle occupancy can be approximately calculated by (1 + number of passengers / number of drivers). More specifically, without joint travel behaviors, the vehicle occupancy for the private car is 1. However, with joint travel behaviors, the vehicle occupancy should be larger than 1. Under the assumption that a joint travel behavior only includes two persons, when the vehicle occupancy is 1.3 person/vehicle, the proportion of joint travel behavior of total demand should then be about 30%.

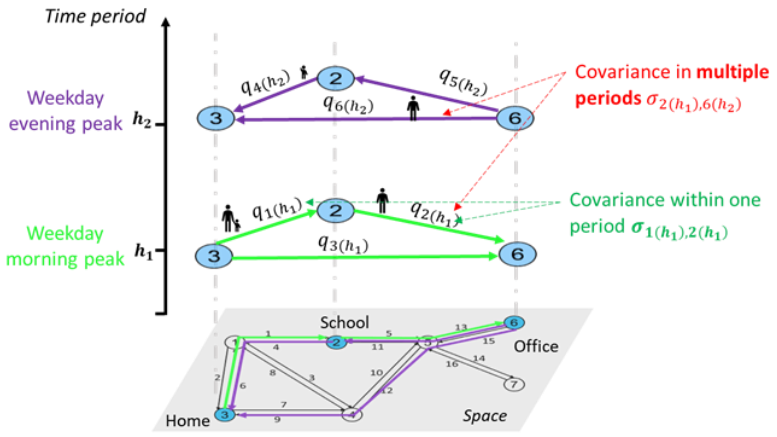

Fig. 1 Different activities and travel patterns in different periods

In this paper, we model the effects of multi-period OD demand covariance on installation of multi-type

sensors including both point and AVI sensors. Point sensors are assumed to be able to count the number of vehicles passing through the link. AVI sensors can only identify the tagged vehicles and match with the records from other locations. The similarity between point and AVI sensors is that both types of sensors can count vehicles at a certain point installed with a sensor. However, they differ in that point sensors can count all vehicles, while AVI sensors can detect (or count) only the portion of vehicles equipped with AVI tags. Another difference is that AVI sensors are also able to cover a spatial area, namely count partial path flows by matching the tagged vehicles at different locations.

In summary, AVI and point sensors provide complementary information. While point sensors can detect complete link flow observation for all vehicles at the installed locations (i.e., point coverage), AVI sensors can detect (i) partial link flow (i.e., point coverage) and (ii) partial path flow for the tagged vehicles (i.e., spatial coverage).

1.4.2 Contributions

With explicit consideration of covariance relationships of various traffic sensor data in multiple periods, this paper proposes a novel model to locate multi-type traffic sensors (point sensors and AVI sensors) for estimation of multi-period OD demands. Generally, the major contributions of this paper can be summarized as follows.

(C1) The **covariances** of multi-period OD flows are explicitly incorporated into the SLP in response to the effects of joint travel behaviors, inter-relationships of the travel patterns in different periods, and major changes in the network topology or land use. For example, as displayed in Fig. 1, the covariance between OD demands during different time periods exists due to the joint travel behavior by the spouse and the child. This joint travel behavior can be evidenced by the average vehicle occupancy larger than 1.4 persons per private car from 7:00 am to 11:00 pm (Transport Department, 2018).

(C2) **Multi-period OD demands**, particularly under congested conditions, should be estimated based on various but co-related traffic sensor data over time because of the time-to-time variation of hourly OD demands. Furthermore, the consequence of traffic congestions for hourly OD demand may carry over into the next hourly period. With taking into account the spatial-temporal covariance of OD demands in multiple time periods, this paper proposes a new model to optimize the multi-type traffic sensor locations for multi-period OD demand estimation.

(C3) In this paper, both the number and locations of **multi-type traffic sensors**, including point sensors and AVI sensors, can be optimized simultaneously. The coordination of different traffic data provided by various sensor types can help to elucidate the inter-relationship of travel patterns over time. The trade-off between these two different sensor types is analyzed to provide more insights into the determination of sensor type priority as analytically demonstrated in Proposition 2 in the model formulation section.

(C4) A more generalized criterion to allocate multi-type traffic sensors for OD demand estimation in multiple periods has been proposed in this paper. By using the proposed model, as proved in Proposition 1, fewer sensors will be needed to achieve a similar quality of OD demand estimates for different time periods, as compared to the results of the previous models.

The rest of this paper is organized as follows. The model assumptions and problem statement are given in Section 2. In Section 3, the relationships between observations from diverse sensor types and OD demand in multiple periods are presented and discussed. Based on these relationships, a PCA-based Kalman filter model is developed with explicit consideration of the covariance of OD demand in multiple periods in Section 4. In Section 5, a generalized model is proposed for multi-type sensor location optimization considering both point and AVI sensors for multi-period OD demand estimation. The mathematical properties of the proposed model are also discussed. In Section 6, three example networks are adopted to demonstrate the insightful findings based on the proposed model. This is followed by the conclusions and suggestions for further studies in Section 7.

2 Model assumptions and problem statement

To focus on the main aims of this paper, the following assumptions are adopted:

(A1) The partial information of prior OD demands and their covariances by hourly period can be obtained and regarded as historical data (Parry and Hazelton, 2012).

(A2) Point sensors and AVI sensors are installed on the selected links in a road network.

(A3) The vehicles equipped with AVI tags are a representative subset of the total vehicles traveling in the road network (Zhou and List, 2010).

Basically, it is assumed that the linear function of observed traffic flow of tagged vehicles is unbiased and can be used to estimate total vehicular flow on this particular link. Two underlying assumptions are included: (i) the AVI sensors can correctly identify each tagged vehicle without matching errors; (ii) the average penetration rate of tagged vehicles over the road network is considered. Note that the penetration rate can vary by location of AVI sensors due to the uncertainties in travel behaviors and traffic demand. However, it is difficult to get the penetration rate for each location of AVI sensors. To clearly demonstrate the key contributions of this paper, an average penetration rate is adopted for the entire network.

For instance, in Hong Kong, there were approximately 785,000 registered vehicles including 167,300 commercial vehicles at the end of 2018. Approximately 350,000 vehicles had been installed with Autotoll tags to enable automatic toll charge payments. Therefore, the overall penetration rate of all tagged vehicles is approximately 45% in Hong Kong.

(A4) The amount of traffic in operation during the studied period is of interest. This means it is possible that OD demands starting before and/or ending after the studied period are taken into account.

The traffic sensor location problem for OD demand estimation contains two main inter-related stages as presented in Fig. 2: (i) multi-type traffic sensor location generation and (ii) multi-period OD demand estimation (Mirchandani et al., 2009; Fei et al., 2013; Hu et al., 2016).

Given the prior OD demand information for a network (represented by nodes, links, and paths), PCA is adopted in this paper to extract the principal OD demand components from the prior OD demand. More specifically, these principal OD demand components can be pre-determined before starting the two-stage model. After performing the PCA, the prior OD demand matrix is divided into principal OD demand components and a matrix of eigenvectors. The former represents the essential features in the original OD demand matrix. The latter stands for a transformation direction between the original OD demand matrix and the principal OD demand component.

At the first stage, the inputs are the network topology and the prior principal OD demand components. Given the total budget, the focus of the first stage is to generate candidate point sensor and AVI sensor locations in the road network. Point sensors can provide counts of all vehicles passing the locations (or roads) installed with this type of sensor. AVI sensors, in addition to the partial link flow data of tagged vehicles, can provide partial path flows by matching records of identified vehicles at different locations.

At the second stage, based on the observations from the traffic sensors planned by the first-stage model, multi-period stochastic OD demands can be estimated. On the basis of these estimates, the uncertainties of the estimations calculated from the total trace of the OD demand matrix and weighted by their covariance values can be evaluated. The calculated uncertainties of OD demand estimates serve as a feedback mechanism so that the candidate sensor location scheme will then be adjusted accordingly. By comparing the uncertainties of OD demand estimates among all of the candidate traffic sensor location schemes using the firefly algorithm (Fu et al., 2019), the optimal scheme contributing to the minimum uncertainty of multi-period OD demand estimates can be selected.

The problem studied at the second stage is to estimate the multi-period OD flows from measured link/path flows by using network and path choice models. Specifically, the second-stage problem for OD demand estimation is indeed a bi-level problem, as shown in Fig. 2 (Bierlaire, 2002; Cascetta, 2009; Jones et al., 2018). The upper level, given that the link/path choice proportion matric is known, estimates OD demand with observed link flows obtained from point sensors and partial path flows obtained from the AVI sensors. The lower level updates the link/path choice proportions by assigning the OD demand estimated in the upper level by using an adapted traffic flow simulator (which is developed based on stochastic user equilibrium (SUE)) (Lam and Xu, 1999). The link and path flow obtained from the adapted traffic flow simulator at the second stage should be consistent with the observed ones from traffic sensors. Thus, the bi-level OD estimation model iterates until the difference between the estimated link/path flow from the adapted traffic flow simulator and observed link/path flows from traffic sensors is less than the predetermined tolerance.

During iterations of the two-stage model, the proposed multi-period OD demand estimation model at the second stage updates the values of principal OD demand components. Taken directly from these principal OD demand components, the OD demand matrix can then be inferred based on the eigenvectors extracted by the PCA procedure. Note that these eigenvectors do not change during the iterative process and the PCA only needs to perform once.

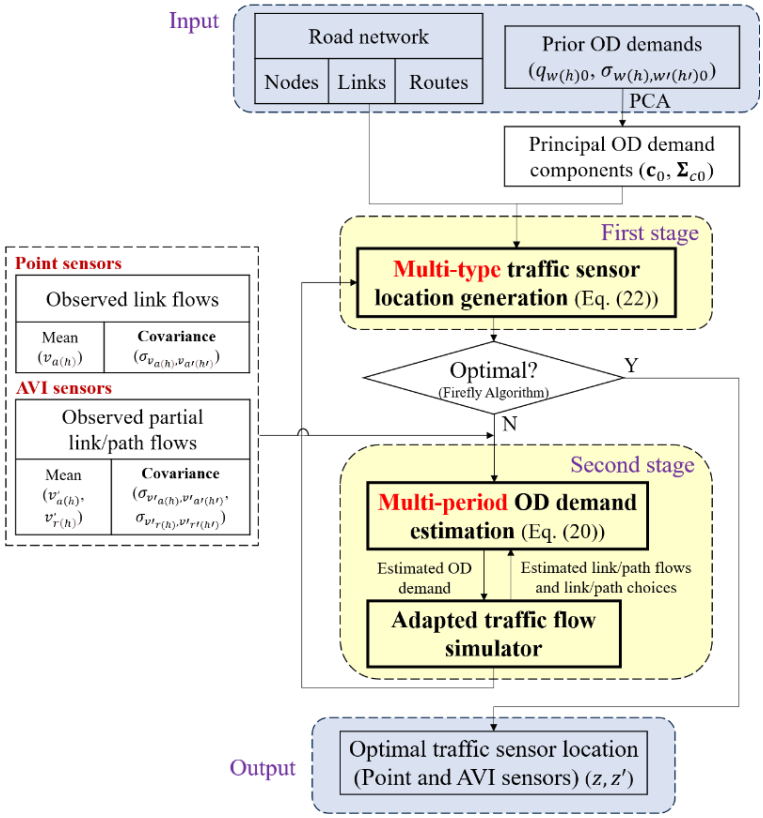

Fig. 2 The flowchart of the traffic sensor location model

3 Relationship between observations and multi-period OD demand estimation

In this paper, some typical hourly periods have been chosen to reflect the variation of travel patterns during multiple periods over the year. It should be noted that before proceeding with model formulations, the complete notations for all of the variables and parameters can refer to the Appendix D for a global view. Consider a road network with a set of links **A,** set of OD pairs **W**, and set of paths or path segments **R**. The determinant function $|\cdot|$ of the set represents the number of the corresponding network features. For instance, $|\mathbf{A}|$ means the number of links in the road network. The typical periods denoted as a set **H** in this paper include the morning peak hour (i.e., 8:00–9:00) and the evening peak hour (i.e., 17:00–18:00) on weekdays together with a typical peak hour (i.e., 12:00–13:00) on weekends.

The **observations** include those from both point and AVI sensors. Specifically, for point sensor observations, $v_{a(h)}$ represents the mean of observed hourly traffic flow on link a from point sensors in period h. $\sigma_{v_{a(h)},v_{a'(h')}}$ represents the covariance of observed hourly traffic flow between link flows v_a during period h and $v_{a'}$ during period h' by point sensors. For AVI sensor observations, $v'_{a(h)}$ stands for the mean of observed partial hourly traffic flow on link a by an individual AVI sensor in period h. $v'_{r(h)}$ stands for the mean of observed partial traffic flow on path or path segment r by a pair of AVI sensors in period h. $\sigma_{v'_{a(h)},v'_{a'(h')}}$ and $\sigma_{v'_{r(h)},v'_{r'(h')}}$ are the covariance of observations corresponding to the partial link flows $v'_{a(h)}$ and partial path flows $v'_{r(h)}$, respectively. The corresponding vector or matrix of the observations (e.g., $\mathbf{v}_{a(h)}$, $\mathbf{v}'_{a(h)}$, $\mathbf{\Sigma}_{v_a}$, $\mathbf{\Sigma}_{\mathbf{v}'_a}$) are boldfaced.

The **unknown variables** needed to be estimated are the mean and covariance of OD demands. $q_{w(h)}$ is

denoted as the traffic demand of OD pair w during period h. $\sigma_{w(h),w\prime(h\prime)}$ is denoted as the covariance estimate of traffic demands between OD pairs w in period h and OD pair w' in period h'. In addition, the decision variables also include the point and AVI sensor location indexes represented by z and z', respectively. Both z and z' are binary variables. The boldface of these observations (e.g., $\mathbf{q}_{(h)}$, $\mathbf{\Sigma}_q$) represents the corresponding vector or matrix.

The sample mean of observed vehicular flow during the period h ($h \in \mathbf{H}$) within a studied year is calculated as

$$\mathbf{v}_{(h)} = \frac{1}{|\mathbf{D}|}\sum_{d\in\mathbf{D}} \mathbf{v}_{(h,d)}\ , \tag{1}$$

where $\mathbf{v}_{(h)} = \left[v_{1(h)}, v_{2(h)}, \ldots, v_{|\mathbf{A}|(h)}\right]^T$ is the column vector of sample mean link flows on all links during time period h, in which $v_{a(h)}$ is the sample mean link flow on link a during time period h. $\mathbf{v}_{(h,d)} = \left[v_{1(h,d)}, v_{2(h,d)}, \ldots, v_{|\mathbf{A}|(h,d)}\right]^T$ is a column vector of traffic flows on all links in period h on day d ($d \in \mathbf{D}$) over the days of interest. $\mathbf{D}$ is the set of days considered, and $|\mathbf{D}|$ is the number of days.

The sample covariance of observed flows among different links during multiple periods within the year is calculated as

$$\Sigma_v = (\sigma_{v_a(h),v_{a'}(h')})_{mr\times mr} = \frac{1}{|\mathbf{D}|-1}\sum_{d\in\mathbf{D}}\{(\mathbf{v}_{(d)}-\mathbf{v})(\mathbf{v}_{(d)}-\mathbf{v})^T\}, \tag{2}$$

where $\sigma_{v_a(h),v_{a\prime}(h\prime)}$ represents the sample covariance between vehicular flows on the links a in period h and a' in period h', respectively. $\mathbf{v}$ is a vector of mean hourly traffic flow during all periods obtained by vertically concatenating $\mathbf{v}_{(h)}$, $\mathbf{v} = (\ldots(\mathbf{v}_{(h)})^T\ldots)^T$. $\mathbf{v}_{(d)}$ is a vector of traffic flows on all links during all periods of interest on day d ($d \in \mathbf{D}$) obtained by vertically concatenating $\mathbf{v}_{(h,d)}$, $\mathbf{v}_{(d)} = (\ldots(\mathbf{v}_{(h,d)})^T\ldots)^T$.

3.1 Observation from point sensors

As described in section 1.3, point sensors supply entire traffic flows on selected links in a road network, including their mean and covariance. The observed traffic flows on link a during period h can be expressed by the OD demands and link choice proportions.

$$v_{a(h)} = \sum_{w\in\mathbf{W}} p_{aw(h)}q_{w(h)} \quad \forall a \in \mathbf{A}, h \in \mathbf{H}\ , \tag{3}$$

where $p_{aw(h)}$ is the link choice proportion of OD pair w passing through link a in period h. $q_{w(h)}$ is traffic demand in OD pair w during period h. For any link installed with a point sensor in any time period, the Eq. (3) means that the observed link flow by a point sensor ($v_{a(h)}$) equals the summation of OD demand passing through this link ($\sum_{w\in\mathbf{W}} p_{aw(h)}q_{w(h)}$).

The covariance between the observed link flows v_a during period h and $v_{a\prime}$ during period h' can be obtained as follows:

$$\sigma_{v_a(h),v_{a'}(h')} = \sum_{w' \in \mathbf{W}} \sum_{w \in \mathbf{W}} p_{aw(h)} p_{a'w'(h')} \sigma_{w(h),w'(h')} \quad \forall a, a' \in \mathbf{A}, h, h' \in \mathbf{H}, \tag{4}$$

where $\sigma_{w(h),w\prime(h\prime)}$ is the covariance estimate of traffic demands between OD pairs *w* in period h and w' in period h'.

For simplicity, Eqs. (3) and (4) are expressed in the matrix form:

$$\mathbf{v}_{(h)} = \mathbf{P}_{(h)} \mathbf{q}_{(h)}, \text{ and} \tag{5}$$

$$\Sigma_v = \mathbf{P} \Sigma_q (\mathbf{P})^T. \tag{6}$$

3.2 Observation from AVI sensors

From the assumption (A3), the penetration rate of tagged vehicles can serve as a representative index of all vehicles, allowing one to estimate path flow and OD demand even though only those tagged vehicles can be matched by AVI sensors.

To estimate the OD demands using observations from AVI sensors, two different cases can be summarized as follows, based on the information observed by (I) only one AVI sensor and (II) more than one AVI sensor.

(I) Similar to point sensors, the information obtained from an individual AVI sensor in period h can be used for OD estimation as follows:

$$v'_{a(h)} = \pi \cdot \sum_{w \in \mathbf{W}} p_{aw(h)} q_{w(h)} \quad \forall a \in \mathbf{A}, h \in \mathbf{H}. \tag{7}$$

$v'_{a(h)}$ is the observation from an individual AVI sensor on link *a*. $q_{w(h)}$ is the unknown OD demand of OD pair *w* in time period *h* needed to be estimated. $p_{aw(h)}$ is the link choice proportion that represents the proportion of OD demand of OD pair *w* in time period *h* going through link *a*. The link choice proportion is assumed to be known in the upper level of the OD demand estimation problem, while this proportion will be updated by a traffic flow simulator (which is developed based on SUE) at the lower level with a given OD demand. π is the average penetration rate of tagged vehicles. Specifically, for link *a* equipped with a point sensor and an AVI sensor, partial link flows passing through (v_a) together with the number of tagged vehicles (v'_a) can both be observed. The penetration rate for tagged vehicles on link *a* can then be estimated from $\pi_a = v'_a / v_a$. Therefore, the average penetration rate for tagged vehicles for all links equipped with AVI sensors π can be calculated.

For any link installed with an AVI sensor in any time period, the Eq. (7) holds and is used to describe the linear relationship between the observation from the individual AVI sensor $(v'_{a(h)})$ and estimated OD demand $(q_{w(h)})$. An intuitive explanation of Eq. (7) is that the observed partial link flow by an individual AVI sensor $(v'_{a(h)})$ equals the summation of OD demand passing through this link $(\sum_{w \in \mathbf{W}} p_{aw(h)} q_{w(h)})$ multiplied by the penetration rate (π) of tagged vehicles.

(II) The tagged vehicles observed by more than one AVI sensor sequentially can also be used for OD demand estimation considering the penetration rate of tagged vehicles. To incorporate the information obtained from paired AVI sensors, i.e., AVI sensors that identify the same tagged vehicle on different links, the relationship between the observations from paired AVI sensors and OD demand in period h can be described as follows:

$$v'_{r(h)} = \pi \times \sum_{w \in \mathbf{W}} p'_{rw(h)} q_{w(h)} \quad \forall r \in \mathbf{R}, h \in \mathbf{H}, \tag{8}$$

where $p'_{rw(h)}$ denotes the proportion of traffic demand in OD pair w passing through path or path segment r in period h. The path or path segment r is defined by the sequence of traversed AVI sensors. The Eq. (8) means that for any path that can be observed by matching AVI sensors at different locations in any time period, the observed partial path flow ($v'_{r(h)}$) equals the summation of OD demand passing through this specific path ($\sum_{w\in\mathbf{W}} p'_{rw(h)} q_{w(h)}$) multiplied by the penetration rate (π) of tagged vehicles. Note that AVI sensors can also be installed at the entry and exit links before the origin and destination nodes, in which case the relationship between AVI observations and OD demand in period h can be represented as following Eq. (9):

$$v'_{r(h)} = \pi \times q_{w(h)} \quad \forall r \in \mathbf{R}, h \in \mathbf{H}. \tag{9}$$

Furthermore, information including flow and travel time detected by AVI sensors can further improve the estimation of link or path segment choice proportions. Interested readers can refer to Zhou and List (2010) for the update of link choice proportion from observed flow information, and Zhu et al. (2019) for the update of path choice proportion from observed travel time information.

4 Multi-period OD demand estimation

4.1 Principal component analysis for OD demand estimation

The OD demands generated in multiple periods present significant variability in both spatial and temporal manners. For instance, at the morning peak hour on weekdays, most traffic demand is directed from residences to places of work, while the direction of demand is reversed during the evening peak hour. In contrast, on weekends and public holidays, people seldom travel to places of work. When considering multiple periods, the number of OD demand variables needed to be estimated increases dramatically. However, because only a subset of OD pairs is dominant in any specific period, these OD pairs of particular importance can be taken to represent the overall characteristics of all OD pairs.

Using PCA, the dominant OD demands, i.e., those which exhibit the greatest dynamics, can be extracted from the covariance of OD demand in multiple periods (Djukic et al., 2012; Krishnakumari et al., 2020). Mathematically, assuming that there are n OD pairs in a road network and k periods of interest, the traffic demand of OD pair w during period h is denoted as $q_{w(h)}$. We denote a column vector $\mathbf{q_w} = \left[q_{w(h_1)}, q_{w(h_2)}, \ldots, q_{w(h_k)}\right]^{\boldsymbol{T}}$ representing the traffic demands in OD pair w during the observation periods from h_1 to h_k.

As proposed by Djukic et al. (2012), one can extract the essential features of the multi-period OD demand matrix to improve the effectiveness of the method for OD demand estimation and sensor location optimization. The PCA method has been used in this paper to extract the principal OD demand components in multiple periods.

The multi-period OD demand matrix can be written as the following matrix considering the spatial and temporal information of OD demands.

$$\mathbf{q} = \left[\mathbf{q_1}, \mathbf{q_2}, \ldots, \mathbf{q_n}\right] = \begin{bmatrix} q_{1(h_1)} & q_{2(h_1)} & \cdots & q_{n(h_1)} \\ q_{1(h_2)} & q_{2(h_2)} & \cdots & q_{n(h_2)} \\ \vdots & \vdots & \ddots & \vdots \\ q_{1(h_k)} & q_{2(h_k)} & \cdots & q_{n(h_k)} \end{bmatrix}. \tag{10}$$

By reformulating the multi-period OD demand matrix to a column vector $[\mathbf{q_1}^T, \mathbf{q_2}^T, \ldots, \mathbf{q_n}^T]^T$, the covariance matrix of the multi-period OD demand with the size of $(n \times k) \times (n \times k)$, which is real and symmetric, can then be calculated and expressed as follows:

$$\boldsymbol{\Sigma}_{\mathbf{q}} = \begin{bmatrix} \boldsymbol{\Sigma}_{\mathbf{q}(h_1)} & & sym. \\ \vdots & \ddots & \\ \boldsymbol{\Sigma}_{\mathbf{q}(h_1,h_k)} & \cdots & \boldsymbol{\Sigma}_{\mathbf{q}(h_k)} \end{bmatrix} = \begin{bmatrix} \sigma_{1(h_1)} & & & & & & \\ \vdots & \ddots & & & sym. & & \\ \sigma_{1(h_1),n(h_1)} & \cdots & \sigma_{n(h_1)} & & & & \\ \vdots & \vdots & \vdots & \ddots & & & \\ \sigma_{1(h_1),1(h_k)} & \cdots & \sigma_{n(h_1),1(h_k)} & \cdots & \sigma_{1(h_k)} & & \\ \vdots & \ddots & \vdots & \cdots & \vdots & \ddots & \\ \sigma_{1(h_1),n(h_k)} & \cdots & \sigma_{n(h_1),n(h_k)} & \cdots & \sigma_{1(h_k),n(h_k)} & \cdots & \sigma_{n(h_k)} \end{bmatrix}, \tag{11}$$

where $\boldsymbol{\Sigma}_{q(h_1)}$ and $\boldsymbol{\Sigma}_{q(h_k)}$ are the $n \times n$ covariance matrices of OD demand within the period h_1 and h_k, respectively, and $\boldsymbol{\Sigma}_{q(h_1,h_k)}$ is the $n \times n$ covariance matrix of OD demand between periods h_1 and h_k. The entry $\sigma_{w(h),w\prime(h\prime)}$ represents the multi-period covariance of traffic demand between OD pair w in period h and OD pair w' in period h'. $\sigma_{w(h),w\prime(h)}$ represents the spatial covariance between OD pairs w and w' in the same period h. $\sigma_{w(h),w(h\prime)}$ represents the temporal covariance for the same OD pair w between time periods h and h'.

Remark 1

When different OD pairs are assumed to be independent at all times, the covariance matrix of OD demands in Eq. (11) can be simplified as a diagonal matrix, in which diagonal elements are the variances while all other elements are zero:

$$\sigma_{w(h),w'(h')} = 0 \quad \forall w, w' \in \mathbf{W}, w \neq w', and \ \forall h, h' \in \mathbf{H}. \tag{12}$$

Alternatively, when different OD pairs are statistically correlated only within the same period, the covariance matrix of OD demands in Eq. (11) can be simplified as a block diagonal matrix:

$$\sigma_{w(h),w'(h')} = 0 \quad \forall w, w' \in \mathbf{W}, and \ \forall h, h' \in \mathbf{H}, h \neq h'. \tag{13}$$

Remark 2

The elements in the multi-period covariance matrix can be positive, zero, or negative. When the covariance is positive (i.e., $\sigma_{w(h),w\prime(h\prime)} > 0$), the traffic demand of OD pair *w* in period *h* has a positive relationship with that of OD pair w' in period h', and vice versa.

As illustrated in Fig. 1, the statistical covariance relationship between OD pairs (3,2) and (2,6) at the morning peak hour is positive, whereas the covariance between OD pairs (6,2) and (6,3) in the evening peak hour is negative.

However, the incorporation of multi-period statistical OD demands dramatically increases the number of OD demand variables that need to be estimated. Therefore, it is challenging to directly infer the mean and covariance of multi-period OD demand accurately with a limited number of traffic sensors. To take advantage of additional information provided by the spatial and temporal covariance of OD demand in multiple periods, PCA is adopted to extract the essential features of the multi-period OD flow matrix. For instance, if the covariance of traffic flows between OD pair w in period h and OD pair w' in period h' is relatively large, these two OD demands are highly correlated, as shown in Fig. 3. With the

negligible loss of information, we can use only one vector e_i, the eigenvector corresponding to the largest eigenvalue, to represent the traffic demands of these two OD pairs, thereby reducing the dimensionality of the multi-period OD demands.

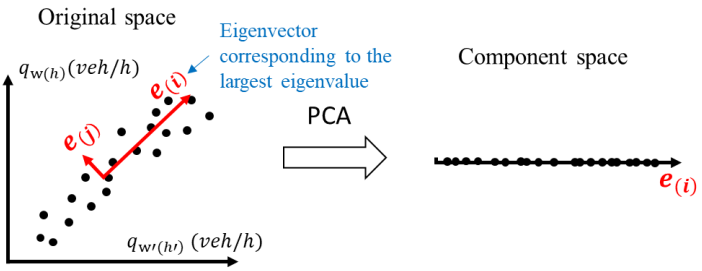

Fig. 3 PCA to extract the principal OD demand components

The eigenvectors of the centered and scaled OD demand covariance matrix contain important information that can be obtained from the singular value decomposition of the covariance matrix. Based on linear algebra, because the $(n \times k) \times (n \times k)$ covariance matrix $\mathbf{\Sigma_q}$ in multiple periods is real and symmetric, the matrix $\mathbf{\Sigma_q}$ can be factorized as follows:

$$\mathbf{\Sigma}_q = \mathbf{\Lambda Y \Lambda}^{-1} \quad , \tag{14}$$

where $\mathbf{\Lambda}$ is the square $(n \times k) \times (n \times k)$ matrix whose column vector is the eigenvector $\mathbf{e_i}$ of $\mathbf{\Sigma_q}$, and $\mathbf{Y}$ is the diagonal matrix whose diagonal elements are the corresponding eigenvalues. The eigenvectors $\{\mathbf{e_1}, \mathbf{e_2}, \ldots, \mathbf{e_{nk}}\}$ of the multi-period OD demand matrix can be considered as an orthonormal basis because the covariance matrix is real and symmetric. Therefore, the centered traffic demands in any OD pair with column-wise zero empirical mean $(\mathbf{q_{w(h)}} - \bar{\mathbf{q}})$ can be expressed by a linear combination of the set of orthonormal vectors as follows:

$$\mathbf{q}_{w(h)} - \bar{\mathbf{q}} = \mathbf{c_1 e_1} + \mathbf{c_2 e_2} + \ldots \mathbf{c_{kn} e_{kn}} = \sum_{i=1}^{kn} \mathbf{c_i e_i} \quad , \tag{15}$$

where c_i is the coefficient of the eigenvector representing the principal OD demand component in the coordinate system. $\bar{\mathbf{q}}$ is the mean OD demand for all OD pairs over all periods. Eq. (15) can be concerned as a simple rotation of the coordinate system from the original OD demands to a new set of coordinates represented by c_i and eigenvectors. By sorting the corresponding eigenvalues in decreasing order, the original OD demand can be retained with M $(M < kn)$ eigenvectors with the maximum variance. Therefore, the information given by the OD demand can be maintained with the least possible information loss after dimensionality reduction by the PCA. A new representation of OD demand with a lower dimension can be expressed as follows:

$$\tilde{\mathbf{q}}_{w(h)} - \bar{\mathbf{q}} = \mathbf{c_i E} \, , \tag{16}$$

where $\tilde{\mathbf{q}}_{\mathrm{w(h)}}$ is the approximate OD demand in period h represented by M eigenvectors and the principal OD components $\{c_1, c_2, \ldots, c_M\}$. $\mathbf{E}$ is the matrix containing all of the eigenvectors.

The principal OD demand components with M dimensions are extracted to capture the main contribution of the original OD demand matrix with $n \times k$ dimensions. The extraction by PCA can potentially make full use of the additional information arising from the consideration of multiple periods. Instead of directly estimating the original traffic demand in all OD pairs, the OD demand estimation problem first shifts the focus to estimating principal OD demand components from traffic sensors. The multi-period traffic sensor location problem becomes that of locating point sensors and AVI sensors to

estimate the principal OD demand components first, then to estimate the traffic demand in all of the OD pairs.

4.2 Multi-period OD demand estimation based on PCA

The multi-period OD demand in a road network can be uniquely represented by the principal OD demand components c_i in the M-dimensional space on the basis of the PCA. By taking account of the measurement errors from point sensors, the relationship between OD demand and observed link flow from point sensors can be represented as follows:

$$v_{a(h)} = \sum_{w \in \mathbf{W}} p_{aw(h)} q_{w(h)} + \varepsilon_a \quad \forall a \in \mathbf{A}, h \in \mathbf{H}, \tag{17}$$

where ε_a denotes the measurement error of traffic flow on link a from a point sensor.

Substituting the principal OD demand components representing the approximate multi-period OD demands into Eq. (17), the following relationship can be obtained:

$$v_{a(h)} = \sum_{w \in \mathbf{W}} \sum_{i=1}^{M} p_{aw(h)} c_i e_i + \bar{v} + \varepsilon_a = \Theta_{(h)} \mathbf{c}_i + \bar{v} + \varepsilon_a \quad \forall a \in \mathbf{A}, h \in \mathbf{H}, \tag{18}$$

where $\Theta_{(h)}$ denotes the matrix of transformed link choice proportion in period h, that is, the transformation of the original link choice proportions to the orthonormal basis matrix of eigenvectors $\mathbf{E}$. $\bar{v}$ is the mean link flow on all links observed by point sensors over all periods.

Furthermore, AVI sensors represent an additional data source to provide path or path segment flows for multi-period OD demand estimation. Based on the principal OD demand components, the observations from AVI sensors in multiple periods can be formulated as follows:

$$\begin{aligned} v'_{r(h)} &= \pi \times \sum_{w \in \mathbf{W}} p'_{rw(h)} q_{w(h)} \\ &= \pi \times \Big(\sum_{w \in \mathbf{W}} \sum_{i=1}^{M} p'_{rw(h)} c_i e_i + \bar{v}' \Big) + \varepsilon'_r \\ &= \pi \cdot \Theta'_{(h)} \mathbf{c}_i + \pi \cdot \bar{v}' + \varepsilon'_r \quad \forall r \in \mathbf{R}, h \in \mathbf{H} \end{aligned}, \tag{19}$$

where $\Theta'_{(h)}$ denotes the matrix of transformed path or path segment choice proportion in period h; that is, the transformation of the original path or path segment choice proportions to the orthonormal basis matrix of eigenvectors $\mathbf{E}$. ε'_r denotes the measurement error of traffic flow on path r from an AVI sensor. $\bar{v}'$ is the mean traffic flow observed by AVI sensors over all periods.

Given the prior information, including mean and covariance of OD demand (i.e., $\mathbf{q}_0$ and $\mathbf{\Sigma}_{q0}$, respectively), the prior principal OD demand components $\mathbf{c}_0$ and their covariance matrix $\mathbf{\Sigma}_{c0}$ can be estimated by PCA. Similarly, the transformed prior link or path choice proportions (i.e., Θ_0 and Θ'_0, respectively) can also be obtained. It is assumed that the measurement errors from point and AVI sensors belong to uncorrelated white noise processes. With the knowledge of the observations from point sensors $\mathbf{v}$ and AVI sensors $\mathbf{v}'$, as well as their variance and covariance matrices from point sensors $\mathbf{\Sigma}_e$ and AVI sensors $\mathbf{\Sigma}'_e$, we can derive the optimal principal OD demand component estimator using a Kalman filter. More comprehensive descriptions of the initial Kalman filter method can be found in Ashok and Ben-Akiva (1993). To combine the information observed from both point and AVI sensors, the following formulation of the Kalman filter is adopted:

$$\mathbf{c} = \mathbf{c}_0 + \mathbf{K}(\mathbf{v} - \Theta_0 \mathbf{c}_0) + \mathbf{K}'(\mathbf{v}' - \pi \cdot \Theta'_0 \mathbf{c}_0) \quad \text{and} \tag{20a}$$

$$\boldsymbol{\Sigma}_c = (\mathbf{I} - \mathbf{K}\Theta_0)(\mathbf{I} - \mathbf{K}'\Theta'_0)\boldsymbol{\Sigma}_{c0} \quad , \tag{20b}$$

where

$$\mathbf{K} = \boldsymbol{\Sigma}_{c0}\Theta_0{}^T(\Theta_0\boldsymbol{\Sigma}_{c0}\Theta_0{}^T + \boldsymbol{\Sigma}_e)^{-1} \quad \text{and} \tag{20c}$$

$$\mathbf{K}' = \boldsymbol{\Sigma}_{c0}\Theta'_0{}^T(\Theta'_0\,\boldsymbol{\Sigma}_{c0}\Theta'_0{}^T + \boldsymbol{\Sigma}'_e)^{-1}. \tag{20d}$$

The above equations are regarded as the update phase in a Kalman filter, where the observations from traffic sensors (i.e., $\mathbf{v}$ and $\mathbf{v}'$), regarded as measurements, are used to update the prior principal OD demand components and obtain their mean by Eq. (20a) and covariance by Eq. (20b). The term $\mathbf{K}$ and $\mathbf{K}'$ are known as the optimal Kalman gain and yield the minimum mean square error of the estimates. $\mathbf{v} - \Theta_0\mathbf{c}_0$ and $\mathbf{v}' - \pi\Theta'_0\mathbf{c}_0$, called the measurement residual, are the errors of the estimate incorporating observed information from point and AVI sensors, respectively.

To improve the efficiency of the solution algorithm, we substitute Eqs. (20c) and (20d) into Eq. (20b). Recall the matrix inversion lemma: given the invertible matrices *A*, *D*, and $D + CA^{-1}B$, we can obtain $(A + BD^{-1}C)^{-1} = A^{-1} - A^{-1}B(D + CA^{-1}B)^{-1}CA^{-1}$, where *A* is an *n*-by-*n*, *D* is a *k*-by-*k*, *B* is an *n*-by-*k*, and *C* is a *k*-by-*n* matrix. Based on this lemma, we can get the following equation:

$$\boldsymbol{\Sigma}_c{}^{-1} = \boldsymbol{\Sigma}_{c0}{}^{-1} + \Theta_0^T\boldsymbol{\Sigma}_e^{-1}\Theta_0 + \Theta'^T_0\,\boldsymbol{\Sigma}'^{-1}_e\,\Theta'_0. \tag{21}$$

The terms $\Theta_0^T\boldsymbol{\Sigma}_e^{-1}\Theta_0$ and $\Theta'^T_0\boldsymbol{\Sigma}'^{-1}_e\Theta'_0$ in Eq. (21) represent the value of the additional information from point sensors and AVI sensors, respectively. Note that the estimation of principal OD demand components and their covariance can be further used to obtain the OD demand in multiple periods by applying Eq. (16) (see Djukic et al. (2012)). Importantly, due to the variation of the multi-period OD demands at different iterations, the link choice proportions are also updated during the OD demand estimation process. This means a bilevel optimization framework is needed for multi-period OD demand estimation especially for congested networks (Zhou and List, 2010). Detailed information on bilevel OD demand estimation can be found in Shao et al. (2014). An adapted traffic flow simulator has been used in this paper to update the link choice proportions in multiple periods (Lam and Xu, 1999).

5 Multi-period traffic sensor locations

To account for the hourly and daily variation of traffic flow, traffic sensor locations should be adapted to different situations in various time periods, rather than for one single period as typically considered in the literature. In this paper, for multi-period OD demand estimation, the number, type, and locations of traffic sensors can be optimized simultaneously while considering the budget constraint.

As stated in Section 4, if link flows are available after the installation of traffic sensors, the principal OD demand components and the multi-period OD demand can be estimated using the Kalman filter. However, for the traffic sensor location problem, it is impossible to observe the link flows from traffic sensors in the planning stage before installation of the sensors. To deal with this, we notice from Eq. (21) that the covariance matrix of the principal OD demand components can be estimated based solely on the traffic sensor locations and without exact observations from the sensors (Zhou and List, 2010; Simonelli et al., 2012). In other words, the *variation* of the multi-period OD demand estimates can be obtained before installing any sensors.

In addition to the variance information, the additional information provided by the covariance of OD demand in multiple periods can also help to optimize the traffic sensor locations and estimate the multi-

period stochastic OD demands. For instance, given two OD pairs with relatively large demand covariance in multiple periods, we can statistically infer that these two OD pairs should have a strong linear relationship with each other (Castillo et al., 2008). Therefore, the OD pairs with the greatest demand covariance values between one another should be assigned higher importance for multi-period OD demand estimates. Mathematically, to incorporate both the variance and covariance of OD demand in multiple periods, the summation of absolute values of OD demand covariances between OD pair w and other OD pairs is considered as the weight on OD pair w.

To present the model formulation more clearly, we first define two mapping functions $\Gamma(A)$ and $D(A)$. The function $\Gamma(A)$ obtains a new matrix whose elements are the absolute values of all of the elements in matrix A. The function $D(A)$ obtains a column vector whose elements are the same as the corresponding diagonal elements in matrix A. The mathematical explanations of these functions can be found in Appendix B. In addition, define a $1 \times M$ row vector $\mathbf{I}$ whose elements are all ones. Therefore, the multi-period traffic sensor locations can be modeled by minimizing the uncertainty of the resultant multi-period OD demand estimates, considering the trace of the covariance matrix[1] to be the estimation uncertainty, as follows:

$$\min_{z,z'} \sum_{w\in\mathbf{W},h\in\mathbf{H}} \left(\sum_{w'\in\mathbf{W},h'\in\mathbf{H}} |\sigma_{w(h),w'(h')}| \right) \sigma_{w(h)}$$
$$= \min_{z,z'} [\mathbf{I} \cdot \Gamma(\mathbf{\Sigma}_c) \cdot D(\mathbf{\Sigma}_c)], \tag{22a}$$

subject to a budget constraint:

$$\beta \sum_{a\in\mathbf{A}} z_a + \beta' \sum_{a\in\mathbf{A}} z'_a \le B, \tag{22b}$$

where z_a and z'_a are binary variables representing point sensor locations and AVI sensor locations, respectively. $z_a = 1$ means that a point sensor is installed on link a, $z'_a = 1$ if an AVI sensor is installed on link a, and both z_a and z'_a are 0 otherwise. β and β' represent installation and maintenance cost for a point sensor and an AVI sensor, respectively. B refers to the total budget for the sensor installation. The multiplication $\mathbf{I} \cdot \Gamma(\Sigma_c)$ is to calculate the weights of all OD pairs w.

The above traffic sensor location model is used to identify the locations of point sensors and AVI sensors by minimizing the expected uncertainty of the multi-period OD demand estimation. Spatial and temporal covariance are explicitly considered when we estimate the uncertainty of the multi-period OD demands based on the traffic sensor locations. The uncertainty reduction is a measurement of reduction in OD demand variance achieved by considering the observations from point sensors and AVI sensors. It should be noted that estimation uncertainty can refer to the weekly, monthly, and annual changes of the OD demand if we set the time interval as a week, month, and year.

To study the traffic sensor location problem for multi-period OD demand estimation, the following two important propositions are analyzed.

Proposition 1: Effects of multi-period OD demand covariance on the optimum number of sensors
Under congested conditions, the covariances of OD demands among different time periods should be non-zero as clarified in the introduction section. By taking account of the covariance of OD demand in multiple periods, we can then achieve the same uncertainty reduction with fewer sensors than considering

[1] In linear algebra, the trace of a square matrix is the sum of elements on its main diagonal.

the OD demand covariance in one period only or neglecting the covariance completely.

Mathematically, for the purpose of illustration, only one type of sensor (i.e., point sensors) is considered in this proposition. Denote the optimal traffic sensor locations by considering OD demand covariance effects in multiple periods as z^*_{mcov}. Likewise, the corresponding locations by taking into account the covariance of OD demand in single period only are denoted as z^*_{bcov}, and that without consideration of any covariance effect as z^*_{nocov}. Proposition 1 can be expressed mathematically as below:
Given $\mathrm{tr}(\Sigma_c - \Sigma_{c0})$, $\sum z^*_{mcov} \leq \sum z^*_{bcov} \leq \sum z^*_{nocov}$.

The proof of this proposition can be found in Appendix B.

Proposition 2: Trade-off between AVI and point sensors
If the value of additional information from each AVI sensor ($\Theta'^{T}\boldsymbol{\Sigma}'_e{}^{-1}\Theta'$) is smaller than that from the equivalent number of point sensors ($\Theta^{T}\boldsymbol{\Sigma}_e{}^{-1}\Theta$), only point sensors should be chosen for the multi-period OD demand estimation. Conversely, if the value of additional information from each AVI sensor is larger than that from the equivalent number of point sensors, only AVI sensors should be chosen. Otherwise, both AVI and point sensors are needed.

The mathematical explanation and proof of Proposition 2 can be found in Appendix C.

5.1 Solution algorithm

The multi-period OD demands and the spatial and temporal covariance information have been explicitly considered in the development of a solution algorithm to solve the proposed SLP. By taking advantage of this additional valuable information, sensor locations can be optimized for the estimation of more accurate multi-period OD demands. It should be remarked that the proposed multi-period traffic sensor location model in formulation (22) is an integer programming model, in which binary decision variables stand for the point and AVI sensor locations. The proposed SLP is NP-hard so that no optimization algorithm can guarantee a global optimum solution, especially for a large-scale problem. Therefore, some meta-heuristic algorithms, such as a variable neighborhood search algorithm, genetic algorithm, or evolutionary algorithm, should be adopted to efficiently solve the proposed SLP.

Inspired by the social behavior of fireflies, a prevailing nature-inspired algorithm, firefly algorithm (FA), was newly developed by Yang (2008) for optimizing continuous problems. This was then extended to other fields such as the mixed integer programming problem (Sayadi et al., 2010; Jati and Suyanto, 2011). As demonstrated in Pal et al. (2012) and Fu et al. (2019), there are three main reasons to support the use of FA to solve the proposed model: (i) high efficiency to solve complex problems; (ii) low time complexity; (iii) includes not only a self-improving process with the current space, but also improvement among its own space from the previous stages. In our paper, we further adapt this FA to deal with the proposed SLP, which is considered as an integer programming problem. FA techniques are multipoint searching methods, potentially having global and probabilistic search capabilities. Additionally, the role of starting the initial search around the apriori demand plays an important characteristic in building the initial population to efficiently solve the SLP. The efficiency and effectiveness of the adapted FA for solving the proposed SLP will be examined by numerical examples.

In the FA framework, the point sensor and AVI sensor location schemes can be conveniently represented by a firefly analogy. Specifically, $\mathbf{z}$ and $\mathbf{z'}$ are vectors whose elements are binary variables having allowable values of 1 or 0 only. The adapted FA is to decide the values of all elements in $\mathbf{z}$ and $\mathbf{z'}$. The objective of the traffic sensor location model is represented by the light intensity of the fireflies (i.e., $In(\mathbf{z}, \mathbf{z'}) = \mathbf{I} \cdot \Gamma(\mathbf{\Sigma}_c) D(\mathbf{\Sigma}_c)$), which is regarded as the fitness function. In the modified firefly algorithm, light absorption coefficients α_{m} and α_{cov} corresponding to the estimation accuracy of the mean and covariance of multi-period OD demand are defined. A more accurate OD demand estimate in the previous iteration will lead to a larger light absorption coefficient. These light absorption coefficients are considered as the weights on the attractiveness of fireflies. A smaller light intensity indicates a larger likelihood that the represented sensor location schemes will be selected. The attractiveness of a firefly is proportional to its brightness, which is determined by the fitness function. Attractiveness and distance are determined as in Fu et al. (2019).

Algorithm steps

Step 0 (Preprocessing)

Map the prior multi-period OD demand by utilizing the adapted traffic flow simulator to obtain prior link choice proportions $\mathbf{P}_{0(h)}$ and path or path segment choice proportions $\mathbf{P'}_{0(h)}$ in all periods. Perform the PCA for the prior multi-period OD demands to obtain $\mathbf{c}_0$ and $\mathbf{\Sigma}_{c0}$. Calculate the relevant Θ_0 and Θ'_0 as shown in Eqs. (18) and (19).

Step 1 (Initialization)

Randomly generate the initial point sensor and AVI sensor locations ($\mathbf{z_0}$ and $\mathbf{z'_0}$, respectively) on the basis of the budget constraint. The maximum generation (or iteration) is set to T, and the current iteration is initialized as $t = 0$ (Nayeem et al., 2014). Define the light absorption coefficients α_{m} and α_{cov} corresponding to the estimation accuracy of mean OD demand and multi-period covariance of OD demand, respectively. Define the step size parameter β.

Step 2 (Stopping criterion)

The algorithm will terminate and output the optimal solutions under one of the following conditions:

(a) the gap of objective values between two successive iterations is not larger than the predetermined threshold.

(b) the iteration number exceeds the maximum iteration (i.e., $t > T$).

Otherwise, move on to step 3.

Step 3 (Selection operation)

For each firefly $\mathbf{z_{(t)}}$ and $\mathbf{z'_{(t)}}$, calculate the uncertainty of estimation (using formulation (20)), transform the estimation of principle OD demand components to multi-period OD demand by applying Eq. (16) and update the link choice proportions by the adapted traffic flow simulator, then solve the problem (22). On the basis of the calculated light intensity $In(\mathbf{z_{(t)}}, \mathbf{z'_{(t)}})$, the local optimum ($\mathbf{z}^*_{(t)}$) can be determined by ranking the fireflies.

Step 4 (Variation operation)

Vary the attractiveness of fireflies $\mathbf{z_{(t)}}$ and $\mathbf{z'_{(t)}}$ on the basis of light intensity, light absorption coefficients, and the distance between fireflies. The attractiveness is directly proportional to the light absorption coefficient and light intensity, but inversely proportional to the distance. Update $\mathbf{z_{(t)}}$ and $\mathbf{z'_{(t)}}$ consisting of m individuals according to their attractiveness (i.e., $\mathbf{z_{(t+1)}} = \mathbf{z_{(t)}} + \mathrm{e}^{-(\alpha_{\mathrm{m}}+\alpha_{\mathrm{cov}})\mathbf{r}}(\mathbf{z}^*_{(t)} - \mathbf{z_{(t)}}) + \beta^i$). Update the iteration indicator $t = t + 1$, then move back to step 2.

6 Numerical examples

In this section, three example networks are examined to demonstrate the effectiveness and efficiency of the proposed methodology of the SLP for multi-period OD demand estimation. Efficiency reflects that the optimum sensor location scheme can be achieved by the proposed model with the most accurate multi-period OD demand estimates. Effectiveness defines the ability of the proposed model for solving the SLP for both small and medium-size road networks. Examples 1 and 2 aim to numerically demonstrate the contributions of this paper, as described in subsection 1.4.2, while example 3 is to further explore the effects of joint travel behavior through empirical data collected in Hong Kong. The main experiments are listed as follows:

Example 1

(1) The effects of the covariance of multi-period OD demand on the SLP.
The covariance of OD demand, especially in multiple periods, can significantly affect the results of OD estimation and traffic sensor locations because of the variation of joint travel behaviors over a period of time.

(2) Benchmark comparison among different sensor location models.
The results of sensor locations and OD demand estimation can vary significantly depending on different sensor location models in which whether one-period or multi-period OD demands in SLPs are considered particularly under congested conditions.

(3) The effects of traffic congestion on multi-period OD demand estimation.
Traffic congestion can last a long time and impact travel patterns and OD demands in different periods.

Example 2

(4) The efficiency of multi-type traffic sensors for OD demand estimation.
Partial path and even OD flows observed by AVI sensors can be regarded as a supplement to entire link flows only on selected links provided by point sensors for OD demand estimation. These multi-source data from different sensor types can cooperate with each other to clarify the variation and correlation relationship of multi-period OD demand.

(5) Sensitivity analysis of the cost ratio between point and AVI sensors.
The cost ratio between point and AVI sensors also affects the determination of the budgetary allocation for these different sensor types.

(6) Sensitivity analysis of the number of principal OD demand components.
The PCA method is used for stochastic OD demand estimation to take full advantage of the additional information obtained from the covariance of OD demand, especially in multiple periods. The number of principal OD demand components must be predetermined and can affect the estimation results.

Example 3

(7) Effects of joint travel behavior on the traffic sensor location problem.
Joint travel behavior is one of the key factors contributing to the covariance of OD demand in multiple periods. Based on empirical data in Hong Kong, the effects of travel behavior patterns on multi-type traffic sensor locations are explored.

(8) Convergence test of the solution algorithm.
The convergence of the solution algorithm is tested in this numerical example to demonstrate the effectiveness of the adapted FA.

6.1 A small-size transportation network: Example 1

A small-size road network as exhibited in Fig. 4, consists of 7 nodes, 16 links, and 12 OD pairs. The OD demands in three different periods, including the weekday morning peak (8:00–9:00), weekday evening peak (17:00–18:00), and peak hour on Sunday (12:00-13:00), are considered in this example. Note that it is not necessary to incorporate the afore-mentioned periods only, any period can be included in our proposed model; however, in this example, we adopt these three periods for illustration.

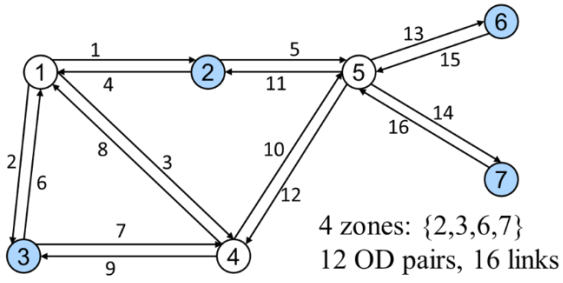

Fig. 4 Example 1 network

For validation purposes, the "true" OD flows, including mean and covariance in multiple periods, shown in Tables 1 and 2, are assumed to be known and are obtained using the re-sampling method (Cascetta and Nguyen, 1988; Lo et al., 1996). Specifically, the "true" hourly OD demands during three different periods over a sequence of days (e.g., 365 days) are simulated from a multivariate normal distribution with desired mean, coefficient of variation, and coefficient of correlation. In this example, the desired mean and coefficient of variation correspond to data provided by the Hong Kong Annual Traffic Census. The desired coefficients of correlation are assumed according to plausible travel behaviors in the road network. The OD demands are then re-sampled with a sampling fraction of 10% so that the mean, variance, and covariance of multi-period OD demands, considered the "true" OD demand information, can be obtained.

On the basis of true multi-period OD demands, the observation of link flows from point or AVI sensors and partial path flows from AVI sensors can be simulated using an adapted traffic flow simulator. Note that to avoid the need to spend too much computation time searching for the feasible paths of the OD pairs, the path set in the road network is predetermined and fixed. The parameters in the traffic flow simulator are identical to those in Lam and Xu (1999).

In this example, the prior multi-period OD flows are set to have the following relationship with true ones: $q_{w(h)0} = (1 - \mu \cdot cv_{w(h)}) \cdot q^*_{w(h)}$ and $\sigma_{w(h),w\prime(h\prime)0} = (1 - \mu \cdot cv_{w(h)})(1 - \mu \cdot cv_{w\prime(h\prime)}) \cdot \sigma^*_{w(h),w\prime(h\prime)}$, where $q^*_{w(h)}$ and $\sigma^*_{w(h),w\prime(h\prime)}$ are the simulated true mean OD demand for OD pair w in period h and the covariance of OD demand between OD pairs w in period h and w' in period h', μ is an independent random variable following a normal distribution $N(0,1)$, and $cv_{w(h)}$ represents the coefficient of variation of the true traffic flows for OD pair w during period h (Yang et al., 1992). The initial link choice proportions for each OD pair are simulated using the stochastic user equilibrium traffic assignment model with the dispersion parameter set to be $\theta = 0.2$. In practice, except for the covariance information, the prior OD demand information can be obtained from surveys or previous models. Furthermore, in a road network with existing traffic sensors or other data sources, prior

information including covariance information can be inferred and updated directly from the available data for more accurate estimation, especially when considering multiple periods.

As an extension to Zhou and List (2010) and Simonelli et al. (2012), we use the percentage of reduction in variance of the multi-period OD demand estimates as the model performance index in this paper. This measurement is more suitable for our case than the others mentioned in section 1.2 because the objective of the proposed model is to determine the sensor locations by minimizing the uncertainty of multi-period OD demand. A smaller uncertainty of OD demand estimates will lead to a larger percentage of reduction in variance, given the prior OD demand information. Hence, the more accurate the multi-period OD demand estimates, the better the sensor location scheme.

Table 1 Assumed true OD demands in multiple periods

OD number	Origin-destination pair	Paths by link number	True mean OD demands		
			Weekday morning peak (h_1)	Weekday evening peak (h_2)	Weekends and public holidays (h_3)
1	2-3	4-2; 4-3-9	168	121	90
2	2-6	4-3-10-13; 5-13	240	180	88
3	2-7	4-3-10-14; 5-14	96	142	110
4	3-2	6-1; 7-8-1; 7-10-11	208	170	120
5	3-6	6-1-5-13; 6-3-10-13; 7-10-13	223	173	115
6	3-7	6-1-5-14; 6-3-10-14; 7-10-14	240	158	280
7	6-2	15-11; 15-12-8-1	144	180	105
8	6-3	15-12-9; 15-12-8-2	168	210	111
9	6-7	15-14	184	151	124
10	7-2	16-11; 16-12-8-1	120	190	185
11	7-3	16-12-8-2; 16-12-9	136	155	171
12	7-6	16-13	208	201	190

Table 2 Assumed true covariance between OD pairs (3,2) and (2,6) in multiple periods

Covariance		Weekday morning peak (h_1)		Weekday evening peak (h_2)		Weekends and public holidays (h_3)	
		(3,2)	(2,6)	(3,2)	(2,6)	(3,2)	(2,6)
Weekday morning peak (h_1)	(3,2)	432.64	339.46	-123.76	37.44	29.95	87.86
	(2,6)	339.46	576.00	40.80	-95.04	34.56	25.34
Weekday evening peak (h_2)	(3,2)	-123.76	40.80	289.00	116.28	85.68	17.95
	(2,6)	37.44	-95.04	116.28	324.00	38.88	66.53
Weekends and public holidays (h_3)	(3,2)	29.95	34.56	85.68	38.88	207.36	121.65
	(2,6)	87.86	25.34	17.95	66.53	121.65	111.51

6.1.1 Effects of covariance of multi-period OD demand on SLP

The covariances of OD demand in multiple periods play a significant role in the OD estimation problem. The effects of multi-period OD demand covariance on the SLP are examined by considering three scenarios:

- Scenario A: No covariance among OD demands.
- Scenario B: Covariance among OD demands only within the same period.
- Scenario C: Covariance among OD demands in multiple periods.

Different covariance relationships among OD pairs are considered in each scenario, but all include three time periods.

In this example, the percentages of reduction in variance achieved by the different traffic sensor location schemes are compared to evaluate the performance of different scenarios. The reduction in variance is represented by the difference in uncertainty between the estimated and prior OD demands (Zhou and List, 2010). The uncertainty is evaluated by the square root of the total trace value for the OD demand covariance matrix. In addition, the mean absolute percentage error (MAPE) of the OD demand estimation is used to evaluate the estimation accuracy based on these scenarios.

Table 3 Effects of OD demand covariance in multiple periods on SLP

Scenario	Covariance consideration	Optimum traffic sensor locations	Percentage of reduction in variance (%)	MAPE (%)
A	No covariance	Point: [3,10] AVI: [4,9,16]	35.66	31.01
B	Covariance only in the same period	Point: [3,5] AVI: [2,9,16]	57.71	17.58
C	Covariance in multiple periods	Point: [3,5] AVI: [2,15,16]	**65.45**	9.88

As indicated in Table 3, the “best” traffic sensor locations depend on the assumptions regarding the covariance relationship of OD demand. It can be seen from Table 3 that in scenario C, where the covariance information in multiple periods is considered, the percentage of uncertainty reduction is 65.45%. Furthermore, the MAPE of OD demand estimation is improved by more than 20% compared with scenario A. Therefore, interestingly, this experiment shows that the consideration of OD demand covariance in multiple periods can efficiently reduce the uncertainty of OD estimates and increase estimation accuracy.

To further gain insights on the performance of the optimum sensor configurations at different levels of covariance, we test the estimation accuracy regarding MAPE based on these three sensor configurations at each level of covariance.

Table 4 Performance of different optimum sensor locations at different levels of covariance

MAPE (%)	Optimum in A Point: [3,10] AVI: [4,9,16]	Optimum in B Point: [3,5] AVI: [2,9,16]	Optimum in C Point: [3,5] AVI: [2,15,16]
A. No covariance	31.03	35.26	32.41
B. One-period covariance	27.19	17.58	20.30
C. Multi-period covariance	**23.05**	**15.51**	9.88

We can observe from Table 4 that when multi-period covariance is taken into account, the MAPE decreases to 23.05% under the sensor configuration of the optimum in scenario A, and changes to 15.51% under the sensor configuration of the optimum in scenario B. The results in Table 4 testify again that even though different optimum sensor configurations are required at different levels of covariance, increasing levels of covariance in OD demands leads to efficient improvement of estimation accuracy. This highlights the need to systematically consider the multi-period covariance of OD demand in SLP.

6.1.2 Benchmark comparison among different sensor location models

For benchmark comparison, the chosen models include model I proposed in Hu et al. (2016), model II proposed in Simonelli et al. (2012), and model III proposed in Fu et al. (2019). The reason why these three models are chosen is that these three models fully cover different types of sensor location models in the literature. Specifically, with respect to the sensor location problem (SLP) for OD demand estimation, existing models can be categorized into three types:

(i) SLP with consideration of the mean OD demand only (Yang and Zhou, 1998; Bianco et al., 2001; Hu et al., 2016),

(ii) SLP with taking into account the mean and variance of OD demand (Zhou and List, 2010; Simonelli et al., 2012), and

(iii) SLP considering mean, variance, and covariance of OD demand in one time period (Fu et al., 2019).

However, to better capture the joint travel behaviors and variation of travel patterns in multiple periods, the covariance of OD demands in multiple time periods should also be incorporated in SLP. The proposed model in this paper fills the gap and is regarded as the fourth category, (iv) SLP with taking into account the mean, variance, and covariance of OD demand in multiple periods.

These existing models (e.g., modes I, II, and III) focus on the estimation of one-period OD demand (e.g., morning peak hour). For comparison of OD demand estimation accuracy in different time periods, the optimum sensor locations for the morning peak hour h_1 in these previous models will be used for OD demand estimation in other time periods. It should be noted that the models proposed in Simonelli et al. (2012) and in Fu et al. (2019) would optimize the locations of point sensors only. In this experiment, we maintain the same settings (e.g., sensor type, time period of interest) consistent with these existing models. When multi-type sensors are used, the cost ratio between point and AVI sensors is set to 1:2 based on the cost data from the Speed Map Panel project in Hong Kong (Transport Department, 2021).

Table 5 displays that with respect to the OD demand estimation accuracy, model IV proposed in this paper contributes to the best sensor locations with the largest average percentage of reduction in variance (**65.45%**) and smallest average MAPE (**9.88%**) for different time periods. This finding can be elucidated

as that model IV explicitly takes into account the mean and covariance of OD demand in multiple periods when determining the multi-type sensor locations. As a result, more available data from multi-type traffic sensors including mean and covariance of multi-period traffic counts can be incorporated. The other three existing models, however, spotlight one of the most congested periods (e.g., morning period h_1). The observed information has not been fully utilized when allocating traffic sensors for estimation of single-period OD demand. The OD demand uncertainty and correlation in different time periods can only be captured by the proposed model IV.

It can also be found in the above Table 5 that the largest percentage of reduction in variance (**79.31%**) is achieved by model II in time period h_1 because the outstanding feature of model II is to reduce the uncertainty of OD demand in the period of interest. This model II puts the effort into decreasing the variation of OD demand in a specific time period by the installation of additional sensors. Furthermore, the best MAPE of OD demand estimates in time period h_1 is **5.42%** resulted from model III. Model III determines the sensor locations by directly minimizing the OD demand estimation error with consideration of covariance of vehicular demand among different OD pairs in the single period of interest. On the other hand, model I is particularly applicable to the situation without any prior traffic flow information even though it is not accomplished in the improvement of OD demand estimation accuracy.

Table 5 Benchmark comparison for sensor location and OD estimation problems

Consideration of OD demand	Optimum traffic sensor locations	Period	Percentage of reduction in variance (%)	MAPE (%)
Model I (Hu et al., 2016)	Point: [7,13] AVI: [5,6,14]	h_1	5.01	20.85
		h_2	3.94	32.47
		h_3	3.26	29.34
		Average	4.07	27.55
Model II (Simonelli et al., 2012)	Point: [3,5,6, 7,10,12,13,14]	h_1	**79.31**	16.59
		h_2	14.12	28.16
		h_3	9.86	24.23
		Average	34.43	22.99
Model III (Fu et al., 2019)	Point: [1,3,6, 9,11,12,13,14]	h_1	41.79	**5.42**
		h_2	12.43	26.78
		h_3	10.17	23.05
		Average	21.46	18.42
Model IV **(this paper)**	Point: [3,5] AVI: [2,15,16]	h_1	76.08	12.24
		h_2	71.15	11.12
		h_3	49.11	6.27
		Average	**65.45**	**9.88**

In summary, when traffic managers intend to make sufficient use of the information observed from installed traffic sensors in different time periods especially including congested peak hour periods, the

proposed model with considering covariance of multi-period OD demand should be chosen with priority over the other existing SLP models.

6.1.3 Effects of traffic congestion on multi-period OD demand estimation

As explained in subsection 6.1.2, the proposed multi-period model outperforms the single-period model in its own period of h_1 because of the strong correlation among multi-period OD demands, especially during the congestion periods in the daytime. To numerically justify this explanation, we conduct a supplementary experiment for multi-period SLP under uncongested conditions for comparison purposes. To imitate the uncongested conditions such as in the mid-night period denoted as h'_1, we reduce the mean and coefficient of correlation of original OD demand in the period of h_1 by five times to decrease the magnitude and correlation relationship of OD demand.

Table 6 SLP for one period vs SLP for multiple periods under uncongested conditions

Consideration of OD demand	Period	MAPE (%)
Existing model: One-period SLP	h'_1	**25.71**
Proposed model: Multi-period SLP	h'_1	34.64
	h_2	13.17
	h_3	18.25
	Average	**22.02**

Table 6 illustrates that under the specified setting of traffic conditions, the MAPE of OD demand estimates during time period h'_1 in our proposed model is 34.64%, which is larger than that from the existing model (i.e., 25.71%). This result confirms our justifications in the preceding subsection 6.1.2, in which when the multi-period correlation relationship is very weak, the single-period model outperforms the multi-period model in its own period of h'_1. Furthermore, Table 6 proves again that regardless of traffic conditions, the proposed model considering multi-period OD demand outperforms the existing model by improving the average accuracy of the multi-period OD demand estimation regarding MAPE.

6.2 A medium-size transportation network: Example 2

Due to the explicit consideration of multi-period OD demands, PCA is adopted to extract the essential features of the OD demands so as to improve the effectiveness of the solution algorithm. The proposed methods are particularly suitable for a road network with a large number of OD pairs.

As shown in Fig. 5, the Sioux Falls network including 76 links and 24 nodes with consideration of 48 OD pairs is adopted. The corresponding origin and destination nodes are marked with the same color. The periods of interest are the same as those in Example 1. The OD demands in these three periods for each OD pair are set to be 300 veh/hour, 200 veh/hour, and 120 veh/hour, respectively. Other parameters are assumed to be identical to those in Shao et al. (2014). The penetration rate of tagged vehicles detected by AVI sensors is assumed to be 45%. It is assumed that this road network is already equipped with four AVI sensors on links 1, 38, 43, and 70, and four point sensors on links 11, 20, 40, and 62, as also presented in Fig. 5.

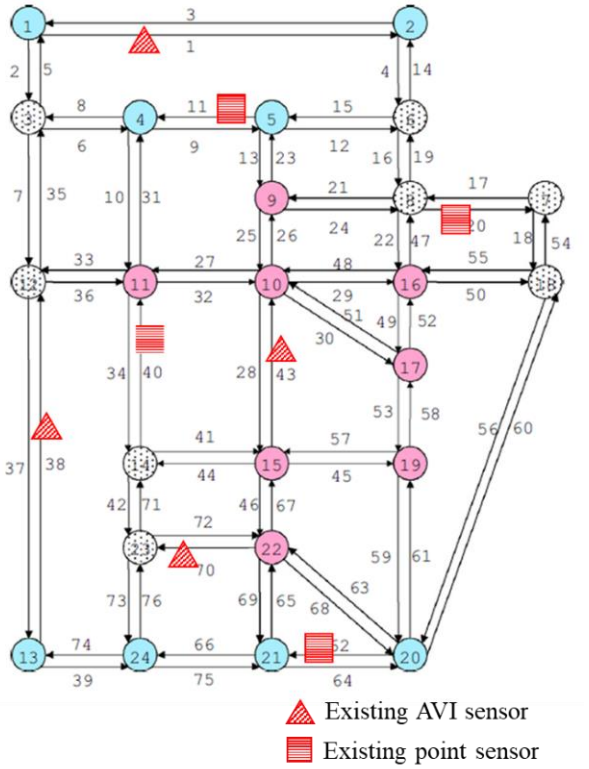

Fig. 5 Example 2 network: Sioux Falls network

6.2.1 Efficiency of multi-type traffic sensors for OD demand estimation

Recall Proposition 2, in which the decision to prioritize AVI sensors or point sensors is determined by the value of additional information obtained when installing these two traffic sensor types, given their relative costs. To provide insight into this proposition clearly and intuitively, the trade-off between AVI sensors and point sensors is examined in this experiment.

In practice, given realistic sensor cost and physical environments, it is difficult to guarantee that an additional AVI sensor can always outperform the equivalent number of additional point sensors concerning OD demand estimation accuracy. Therefore, the efficiency of combining the observations from point sensors and AVI sensors should be further tested. In this experiment, it is assumed that the standard deviations of the measurement errors for point sensors and AVI sensors are 5% and 2.5%, respectively, of the corresponding true traffic flows (Zhou and List, 2010). The unit cost of an AVI sensor and a point sensor is assumed to be β' = \$6,500 and β = \$1,300, respectively. In other words, the unit cost of an AVI sensor is five times that of a point sensor. Given different total budgets, the optimal number and locations of AVI sensors and point sensors are determined based on the proposed models.

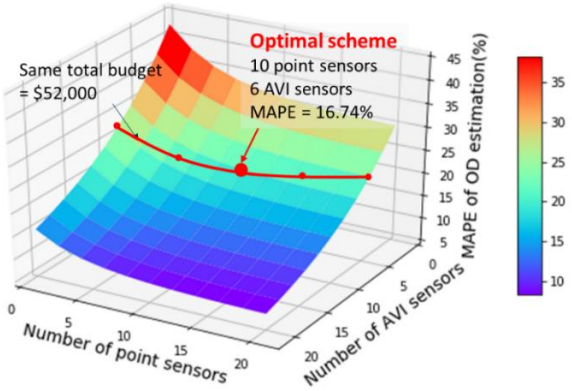

Fig. 6 Efficiency of the combination of point sensors and AVI sensors

From Fig. 6, we can see that when the total budget is $52,000, the optimal traffic sensor location scheme includes 10 point sensors and 6 AVI sensors. The MAPE of OD estimation is then 16.74%, which is the smallest among all location schemes with the same total budget. However, for schemes with only AVI sensors or point sensors, OD estimation accuracy (e.g., 28.81% MAPE for AVI sensors and 20.04% for point sensors) is poorer than that for the combination of information from both sensor types. The results imply that when the measurement errors of AVI sensors and point sensors do not substantially differ, a combination of information from both types leads to a more accurate OD estimation in multiple periods, with smaller MAPE.

6.2.2 Sensitivity analysis of the cost ratio between point and AVI sensors

It has been presented in subsection 6.2.1 that the optimum number and type of traffic sensors are highly dependent on their measurement errors. In addition, because the total budget is usually given and fixed, the cost ratio between AVI and point sensors can also affect the budget allocation for the number of each sensor type. Practically, AVI sensors are normally more expensive than point sensors, as they provide more information and are more reliable. Therefore, the effects of the cost ratio between these two sensor types should be examined to rationalize the budget allocation for the number of each sensor type.

In this experiment, the unit cost of a point sensor is assumed to be fixed (i.e., $\beta = \$1{,}300$). The unit cost of an AVI sensor varies from $\beta' = \$1{,}300$ to $\beta' = \$9{,}100$ so that the cost ratio ranges from 1:1 to 1:7. The total budget is $B = \$31{,}200$. For different cost ratios between point and AVI sensors, we use the proposed model to optimize the number of multi-type traffic sensors and obtain the OD demand estimation results. The MAPEs of the resultant OD demand estimates based on different cost ratios are compared in Table 7.

Table 7 Effects of cost ratio between point and AVI sensors

Cost ratio (point/AVI)	Optimum number of sensors		MAPE (%)
	Number of point sensors	Number of AVI sensors	
1:1	0	24	**4.08**
1:3	6	6	9.17
1:5	9	3	13.61
1:7	24	0	17.93

It is plausible to witness from Table 7 that when the AVI sensor is as cheap as the point sensor, only high accuracy AVI sensors need to be installed in the road network and can contribute to the highest OD demand estimation accuracy with a MAPE of 4.08%. The estimation accuracy regarding MAPE decreases monotonically with the increment of AVI sensor cost. It is also interesting to discover that under the specified settings, the cost ratio between point and AVI sensors smaller than 1/7 makes AVI sensors unattractive. These findings can generally help public agencies to better understand the priority of different sensor types on the basis of their cost ratio, especially for multi-period OD demand estimation.

6.2.3 Sensitivity analysis of the number of principal OD demand components

It has been shown that consideration of covariance in multiple periods can provide additional information for OD demand estimation. To make full and proper use of this additional valuable information, the PCA method is adopted in this paper to improve the effectiveness of the proposed model. However, the number of principal OD demand components must be predetermined. This predetermined variable can also affect the estimation results. Thus, a sensitivity test of the number of principal OD demand components is conducted to elucidate the effectiveness of the PCA method, as presented in Table 8.

In this experiment, it is supposed that four additional point sensors and four additional AVI sensors are to be installed in the road network to cooperate with eight existing traffic sensors. The contribution of the principal OD demand components is calculated as total variances of the selected number of principal OD demand components divided by that of the original OD demands (Jolliffe, 2002).

Table 8 Effectiveness of PCA for the Sioux Falls network

Number of principal OD demand components	Contribution of principal OD demand components	Optimum traffic sensor locations	Percentage of reduction in variance (%)	MAPE (%)	Computation time (s)
25	36.11%	Point: [3,14,45,51] AVI: [5,30,39,66]	21.54	27.14	2,083
50	72.15%	Point: [2,21,44,73] AVI: [10,17,29,60]	53.09	17.66	2,608
82	96.20%	**Point: [2,7,44,51]** **AVI: [10,30,33,61]**	**79.35**	**7.03**	3,705
144	100.00%	**Point: [2,7,44,51]** **AVI: [10,30,33,61]**	**86.13**	**6.10**	12,611

As can be seen from Table 8, with an increasing number of principal OD demand components, the contribution of those components, percentage of reduction in variance, and the computation time all increase, whereas the MAPE decreases monotonically. However, when the number of principal OD demand components increases from 82 to 144, the percentage of reduction in variance does not increase substantially (i.e., from 79.35% to 86.13%), and the reduction of MAPE from 7.03% to only 6.10% is also much smaller than in the other cases. This indicates that when the number of principal OD demand components is large enough, the PCA-based model can guarantee an optimum sensor location scheme and maintain a satisfying level of estimation accuracy.

It is also worth noting that the optimum traffic sensor location scheme ceases to change when the number of OD demand components reaches 82. In this scheme, the point sensors and AVI sensors are located on links 2, 7, 44, and 51, and links 10, 30, 33, and 61. However, computation time increases dramatically with the increasing number of OD demand components, especially when that number exceeds 82. This experiment reveals that even though the PCA-based OD estimation method may lead to partial information loss in multi-period OD demand, it can contribute to sufficiently accurate estimates and significantly reduce computation time, while guaranteeing an optimal scheme of multi-type traffic sensors.

6.3 A transportation network in Hong Kong: Example 3

This numerical example aims to demonstrate the effects of travel behavior patterns on multi-type traffic sensor locations and multi-period OD demand estimation results using empirical data. The Tuen Mun Road Corridor Network in Hong Kong (Fig. 7) is used herein as the study network. The network consists of 487 links, 382 nodes, and 18 zones. These 18 zones include two external zones (S1 and S2) and 16 internal zones (S3-S18) and can be either origins or destinations. Tuen Mun Road (TMR) is an expressway with a higher speed limit compared to Castle Peak Road (CPR) which is a rural road. The internal zones S3-S18 connect only to Castle Peak Road. In the study area, 19 Autoscope point sensors have been installed by Transport Department in Hong Kong to detect traffic flow and travel speed by time of day and day of the year. The weekday morning peak hour and weekday evening peak hour are the two time periods considered in this case study.

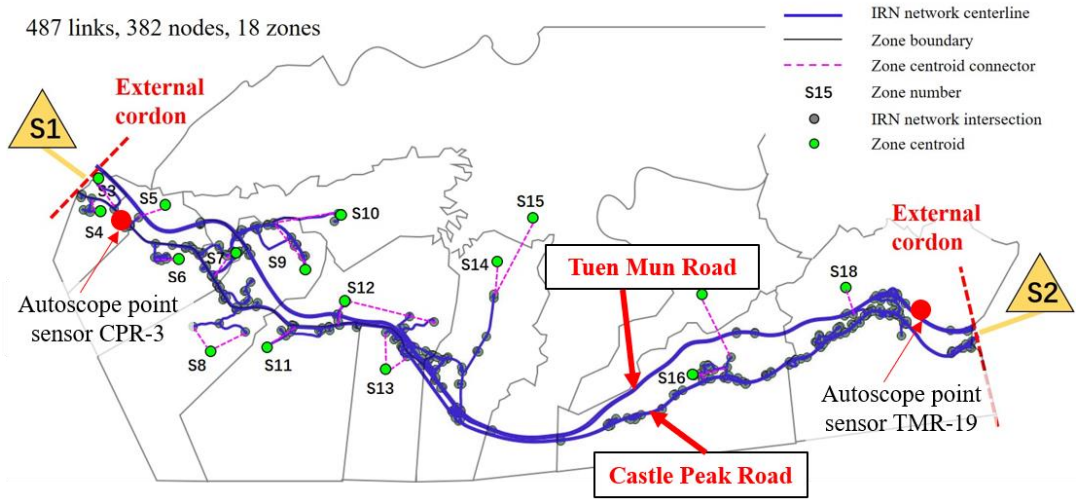

Fig. 7 Example 3 network: Tuen Mun Road Corridor Network in Hong Kong

In this case study, prior OD demand is obtained from Base District Traffic Modal data issued by the Hong Kong Transport Department (Transport Department, 2004) and calibrated using Autoscope point sensors (e.g., control total at external cordons). "True" OD demand is estimated from the data obtained from all available Autoscope point sensors. In the study road network, 9 different link speed-flow curves by link type are calibrated using hourly flow rate and hourly average speed detected by Autoscope point sensors. For instance, Fig.8(a) and (b) show two of these speed-flow curves on Tuen Mun Road and Castle Peak Road calibrated by the data from Autoscope point sensors TMR-19 and CPR-3, respectively. For the link installed with sensor TRM-19, it is found that the capacity is 1,408 veh/hour/lane and the free flow speed

is 70 km/hour. For the location installed with sensor CPR-3, the capacity and free flow speed are 943 veh/hour/lane and 50 km/hour, respectively.

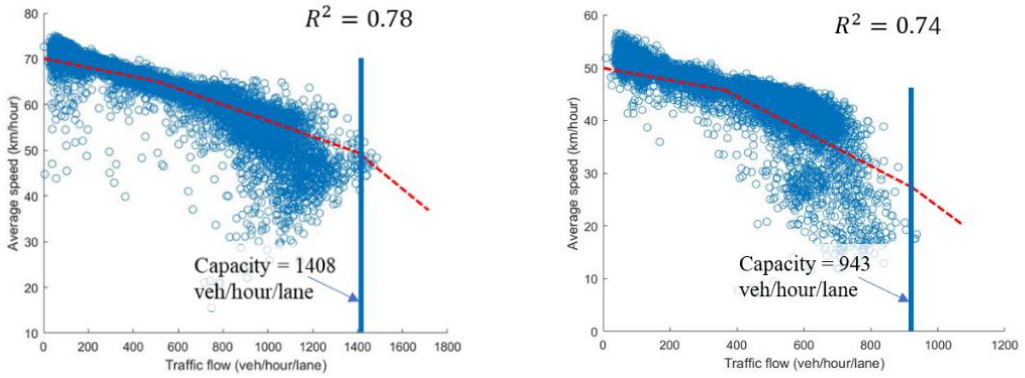

(a) Autoscope point sensor TMR-19 (b) Autoscope point sensor CPR-3

Fig. 8 Speed-flow curves calibrated by data observed from Autoscope point sensors

In this road network, Tuen Mun New Town (S1) and Kowloon Urban Area (S2) primarily serve as the residential area and commercial area, respectively. Some primary schools and kindergartens such as STFA Lee Kam primary school are located in the internal zones S3-S18. The majority of traffic travels from zone S1 to zone S2 in the morning peak hour, while from zone S2 to zone S1 in the evening peak hour.

6.3.1 Effects of joint travel behavior on traffic sensor location problem

As illustrated in the motivating example, joint travel behaviors have significant impacts on OD demand covariance in multiple periods. Consider the travel pattern of a spouse and child similar to the motivating example. Two scenarios (i.e., with and without joint travel behaviors) can be established in the morning peak hour: (i) without joint travel behaviors – the spouse will drive alone from home to the office (S1-S2) and the child will go to school by public transport (only one OD demand from S1 to S2 is generated in this scenario); (ii) with joint travel behaviors – the spouse will drive the child to the school first (S1-an internal zone) and then go on to the office alone (an internal zone – S2) (two OD demands, i.e., one from S1 to the internal zone, the other from the internal zone to S2, will be generated by such joint travel behavior).

The joint travel behaviors can be approximately measured using vehicle occupancy data. According to the reported in "The Annual Traffic Census 2017" of Hong Kong (Transport Department, 2018), vehicle occupancy fluctuates from time to time. As only one sensor in the study area can provide the vehicle occupancy data, it is assumed that vehicle occupancy in the study area remains the same when illustrating the effects of joint travel behavior. In principle, if there is a need to obtain more precise vehicle occupancy data by time and location, a roadside survey can be conducted.

As shown in Fu et al. (2019), the relationship between the covariance of OD demand and the proportion of joint travel behavior of total demands can be theoretically calculated as below. Denote Q_1, Q_2, and Q_3 as the OD demands for (S1-S2), (S1-an internal zone), and (an internal zone-S2), respectively. It is assumed that Q_1, Q_2, and Q_3 are independent normally distributed variables. Denote the proportion of

joint travel of total demands as x, and the standard deviation of Q_1, Q_2, and Q_3 as σ_1, σ_2, and σ_3, respectively. Therefore, the covariance between Q_2 (S1-an internal zone) and Q_3 (an internal zone-S2) could be deduced by the following equation.

$$\mathrm{cov}_{2,3} = x^2 \cdot \sigma_1^2 \tag{23}$$

It can be seen from Eq. (23) that the more joint travel behaviors, the larger the covariance of OD demand between the corresponding OD pairs. Due to the lack of empirical data on the covariance of OD demand, Eq. (23) is used to simulate the prior OD demand covariance based on the proportion of joint travel behaviors.

To demonstrate the effects of travel behavior patterns, the proposed model is implemented under different proportions of joint travel behavior. In this experiment, given the target OD demand estimation accuracy (e.g., MAPE = 10%), the objective is to determine the number and locations of traffic sensors under different proportions of joint travel behavior.

Table 9 Effects of joint travel behavior on optimum number and locations of traffic sensors

Proportion of joint travel behavior	Optimum number of sensors in total	Optimum traffic sensor location scheme	
		Number of sensors on CPR	Number of sensors on TRM
0%	19	6	13
30%	24	12	12
50%	29	19	10
100%	41	33	8

From Table 9, it can be observed that in order to satisfy the target OD demand estimation accuracy, more traffic sensors are needed in view of the increasing number of joint travel behaviors conducted by travelers. It indicates that with more joint travel behaviors, more information is needed for the estimation of both the mean and covariance of OD demand. Therefore, more traffic sensors should be installed to achieve similar accuracy in OD demand estimation.

Table 9 also shows that in this specific study network, when the proportion of joint travel behavior increases, more traffic sensors should be installed on Castle Peak Road. This could be explained by the topology of the study network. Note that the internal zones (S3-S18) are only connected to Castle Peak Road, which is a rural road. As joint travel behaviors will increase the traffic flow on Castle Peak Road (to the internal zones), the covariance between the OD demands of external zone S1 to internal zones (S3-S18) and internal zones to external zone S2 will be enlarged. Thus, more traffic sensors on Castle Peak Road are needed to reduce the uncertainty of the estimated OD demands.

6.3.2 Comparison of performance among different solution algorithms

To solve the proposed problem in this Tuen Mun road corridor network in Hong Kong, there are 974 (487×2) decision variables in the upper-level multi-type sensor location problem leading to mostly 2^{974} potential combinations. For each combination of sensor locations, the lower-level OD demand estimation problem aims to estimate the mean and covariance of traffic demands in 306 OD pairs during different time periods. It is extremely difficult to achieve the global optimum as a result of the large dimension of the problem. Under such a circumstance, meta-heuristic algorithms show their advance to

solve efficiently the study problem with exponential complexity. However, various potential solution algorithms perform differently according to their searching strategies as shown in Table 10. The maximum number of iterations is set to be 100 for each of these different solution algorithms. The performance test is conducted using a laptop computer with an Intel Core i7-2600 CPU, 3.40 GHz, and 8 GB RAM.

Besides the firefly algorithm, however, many other algorithms such as the artificial bee colony algorithm, genetic algorithm are also capable to solve the proposed multi-type sensor location problem. To make the numerical examples more comprehensive, the performance of the modified firefly algorithm has been compared with the original firefly algorithm (Yang, 2008; Fu et al., 2019), genetic algorithm (Salari et al., 2019), and sequential heuristic algorithm (Simonelli et al., 2012) in both Tables 10, 11 and Fig. 9 for benchmark comparison.

Table 10 OD demand estimation accuracy for different solution algorithms

Total number of sensors	Average MAPE for OD demand estimates (%)			
	FA_m*	FA_o	SH	GA
10	15.15	18.53	19.75	32.22
20	9.69	14.17	15.30	24.38
50	**7.91**	12.07	13.14	21.87

* FA_m: modified firefly algorithm; FA_o: original firefly algorithm; SH: sequential heuristic algorithm; GA: genetic algorithm

Table 10 indicates that the modified firefly algorithm proposed in this paper gives the best sensor locations contributing to the most accurate OD demand estimates regardless of the number of sensors. It may benefit from the improved searching strategy in accordance with the OD estimation accuracy at each iteration. The original firefly algorithm and sequential heuristic algorithm can also output satisfying solutions with average MAPE less than 20% even for different numbers of traffic sensors. However, the modified firefly algorithm always outperforms the other existing algorithms used in this experiment.

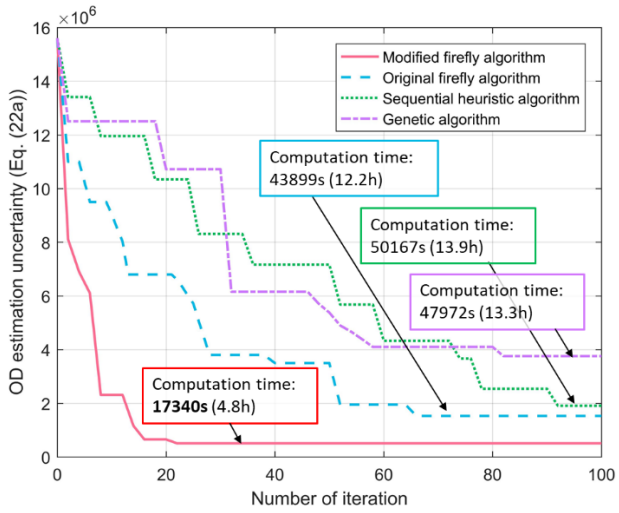

Fig. 9 Performance comparison among different solution algorithms

Table 11 Computational efficiency of different solution algorithms

Algorithm	FA_m*	FA_o	SH	GA
Convergence iteration	**23**	67	141	274
Computation time to converge	17340s **(4.8h)**	43899s (12.2h)	70132s (19.5h)	131852s (36.6h)

* FA_m: modified firefly algorithm; FA_o: original firefly algorithm;
SH: sequential heuristic algorithm; GA: genetic algorithm

As presented in Fig. 9, various solution algorithms (e.g., modified and original firefly algorithms, sequential heuristic algorithm, and genetic algorithm) would lead to totally different optimum solutions of sensor location and corresponding OD demand estimation accuracy. It can be witnessed from Fig. 9 that the modified firefly algorithm can reach the best solution compared to the other three implemented algorithms. Furthermore, the modified firefly algorithm spends the least time 17,340s (4.8h) to converge. Importantly, the results of the other three algorithms presented in Fig. 9 may not be the converged optimal solution. In order to achieve convergence, we do not constrain the maximum number of iterations to investigate the computational efficiency of different solution algorithms. Table 11 shows that the modified firefly algorithm needs the least number of iterations to converge and spends much less time than the other three algorithms for obtaining the optimal solution.

It should be noted that all these solution algorithms cannot guarantee the global optimum solution. However, from the experimental results, the modified firefly algorithm is able to yield the best results within a limited number of iterations as compared to others. Although it spends about 5 hours to solve the case study problem, the computational time required is not a non-trivial issue in this paper as the sensor location problems are usually examined for long-term strategic planning (Fu et al., 2019; Salari et al., 2019).

7 Conclusions and further studies

Due to the within-day and day-to-day variations of traffic demands, the multi-period OD demands are statistically correlated with one another. The effects of OD demand covariance, especially in multiple hourly periods, have become increasingly significant in sensor location problems with different types of traffic sensors under the big data arena.

With a particular emphasis on both spatial and temporal covariance relationships of OD demand, this paper proposes a new model for optimizing multi-type traffic sensor locations. By leveraging sensor data from multiple sources, the uncertainty of multi-period OD demand estimates can be minimized. This paper finds that the considering multi-period OD demand covariance can efficiently reduce the uncertainty of OD estimates and increase the average estimation accuracy regardless of traffic conditions. During congestion periods in the daytime, the multi-period OD demands are highly correlated with one another. As such, it is shown in the numerical examples that the multi-period model outperforms the single-period model even for the OD demand estimates in its own period under congested conditions. In summary, it is recommended to design a multi-type traffic sensor network for multi-period OD demand

estimation and to take into account the multi-period covariance relationship of OD demand, particularly in the congestion periods with uncertainties in traffic demands.

For multi-period OD demand estimation, both the number and locations of multi-type traffic sensors including point sensors and AVI sensors can be optimized simultaneously using the proposed model. We have proven mathematically and numerically that a combination of information from both types outperforms the utilization of single type sensors for multi-period OD demand estimation when the measurement errors of AVI sensors and point sensors do not differ remarkably. Having established that additional data can be provided by multi-period OD demands and multi-type traffic sensors, a PCA-based Kalman filter method was adopted to extract the essential features of the OD demands and enhance estimation efficiency. It has been demonstrated that adoption of PCA can significantly reduce computation time while guaranteeing the optimal location scheme of multi-type traffic sensors.

Further studies should be carried out on heterogeneous traffic sensor location problems while considering multiple-source uncertainties of sensors, such as measurement error and sensor failure, to establish a more reliable sensor network (Hu et al., 2016; Gu et al., 2020). It has also been noted that sensor location problems for travel time inference also deserve investigation considering the practical importance of link and/or path travel time from the aspects of both traffic managers and individual travelers (Yu et al., 2015; Li, 2018; Zhu et al., 2018). Note that the optimal solution of sensor location for OD demand estimation may not be unique, it merits further studies on sensor location problem for multiple purposes such as OD demand estimation and traffic control tasks at the same time (Fu et al., 2019; Sun et al., 2021). Furthermore, it is worth conducting further studies on more efficient solution algorithms for solving the proposed problem in reality for large-scale road networks. The main idea of considering multi-period covariance effects of traffic flow is worthwhile to be extended for traffic management with various vehicle types in a multi-modal transportation network (Wang and Zhang, 2016; Liu et al., 2020; Wang et al., 2020) and in liner container shipping networks (Liu et al., 2014; Meng et al., 2019).

Acknowledgements

The work described in this paper was financially supported by grants from the Research Grants Council of the Hong Kong Special Administrative Region, China (Project Nos. PolyU 152628/16E and R5029-18), National Natural Science Foundation of China (Project Nos. 72071202 and 71671184), Natural Sciences and Engineering Research Council of Canada (NSERC) Discovery, Natural Sciences and Engineering Research Council of Canada (NSERC) CREATE on Integrated Infrastructure for Sustainable Cities (IISC), and Alberta Innovate Strategic Research on Integrated Urban Mobility through Emerging Transportation Technologies.

Appendix A

The matrix calculated from the equation $\Theta_0\boldsymbol{\Sigma}_{c0}\Theta_0^T + \boldsymbol{\Sigma}_e$ in Eq. (20c) is always invertible, with the assumption that the measurement errors on different links are independent and their variances are not equal to zero.

Proof: Note that $\Theta_0\boldsymbol{\Sigma}_{c0}\Theta_0^T = \boldsymbol{\Sigma}_{v0}$ is the covariance of the prior link flows. According to linear algebra,

the covariance matrix $\boldsymbol{\Sigma}_{v0}$ is always positive semi-definite, and thus invertible. In addition, the covariance matrix of measurement error $\boldsymbol{\Sigma}_e$ is positive definite if we assume the measurement errors of different links are independent and their variances are not equal to zero. Therefore, the summation of these two matrices is positive definite, and thus invertible. The proof has been completed.

Appendix B

Proof of Proposition 1

The mathematical expression of Proposition 2 is equivalent to the following.

Given z^*, we can get $tr(\boldsymbol{\Sigma}_c - \boldsymbol{\Sigma}_{c0})_{m\text{cov}} \geq tr(\boldsymbol{\Sigma}_c - \boldsymbol{\Sigma}_{c0})_{b\text{cov}} \geq tr(\boldsymbol{\Sigma}_c - \boldsymbol{\Sigma}_{c0})_{no\text{cov}}$, where $tr(\boldsymbol{\Sigma}_c - \boldsymbol{\Sigma}_{c0})_{m\text{cov}}$, $tr(\boldsymbol{\Sigma}_c - \boldsymbol{\Sigma}_{c0})_{b\text{cov}}$, and $tr(\boldsymbol{\Sigma}_c - \boldsymbol{\Sigma}_{c0})_{no\text{cov}}$ are the uncertainty reductions considering the covariance of OD demand in multiple periods, the covariance in one period, and no covariance, respectively.

First, let us define three mapping functions $\Gamma(A), Diag(A),$ and $BDiag(A,t)$ for matrix A as follows:

$$A = \begin{bmatrix} a_{11} & a_{12} & \dots & a_{1n} \\ a_{21} & a_{22} & \dots & a_{2n} \\ \vdots & \vdots & \ddots & \vdots \\ a_{n1} & a_{n2} & \dots & a_{nn} \end{bmatrix}. \tag{B.1}$$

A is an $n \times n$ matrix.

$$\Gamma(A) = \begin{bmatrix} |a_{11}| & |a_{12}| & \dots & |a_{1n}| \\ |a_{21}| & |a_{22}| & \dots & |a_{2n}| \\ \vdots & \vdots & \ddots & \vdots \\ |a_{n1}| & |a_{n2}| & \dots & |a_{nn}| \end{bmatrix} \tag{B.2}$$

The function $\Gamma(A)$ obtains the absolute values of all elements for matrix A.

$$Diag(A) = \begin{bmatrix} a_{11} & & & \\ & a_{22} & & \\ & & \ddots & \\ & & & a_{nn} \end{bmatrix} \tag{B.3}$$

The function $Diag(A)$ extracts the diagonal elements for matrix A and forms a new diagonal matrix.

$$BDiag(A,t) = \begin{bmatrix} a_{11} & \dots & a_{1t} & & & & \\ \vdots & \ddots & \vdots & & & & \\ a_{t1} & \dots & a_{tt} & & & & \\ & & & \ddots & & & \\ & & & & a_{n-t+1,n-t+1} & \dots & a_{n-t+1,n} \\ & & & & \vdots & \ddots & \vdots \\ & & & & a_{n,n-t+1} & \dots & a_{nn} \end{bmatrix} \tag{B.4}$$

The function $BDiag(A,t)$ extracts the block diagonal elements for matrix A and forms a new block diagonal matrix. The size of each block is t by t.

To prove Proposition 2, recall the matrix inversion lemma, which states that $(A-B)^{-1} = B^{-1}(B^{-1}-A^{-1})^{-1}A^{-1}$.

We can get the following equations:

$$(\boldsymbol{\Sigma}_c - \boldsymbol{\Sigma}_{c0})^{-1} = \boldsymbol{\Sigma}_{c0}^{-1}(\boldsymbol{\Sigma}_{c0}^{-1} - \boldsymbol{\Sigma}_c^{-1})^{-1}\boldsymbol{\Sigma}_c^{-1}$$

$$= -\boldsymbol{\Sigma}_{c0}^{-1}(\Theta_0^T\boldsymbol{\Sigma}_e^{-1}\Theta_0 + \Theta'^T_0\,\boldsymbol{\Sigma}'^{-1}_e\,\Theta'_0)^{-1}\boldsymbol{\Sigma}_c^{-1}$$
$$= -\boldsymbol{\Sigma}_{c0}^{-1}(\Theta_0^T\boldsymbol{\Sigma}_e^{-1}\Theta_0 + \Theta'^T_0\,\boldsymbol{\Sigma}'^{-1}_e\,\Theta'_0)^{-1}(\boldsymbol{\Sigma}_{c0}^{-1} + \Theta_0^T\boldsymbol{\Sigma}_e^{-1}\Theta_0 + \Theta'^T_0\,\boldsymbol{\Sigma}'^{-1}_e\,\Theta'_0)$$
$$= -\boldsymbol{\Sigma}_{c0}^{-1}(\Theta_0^T\boldsymbol{\Sigma}_e^{-1}\Theta_0 + \Theta'^T_0\,\boldsymbol{\Sigma}'^{-1}_e\,\Theta'_0)^{-1}\boldsymbol{\Sigma}_{c0}^{-1} - \boldsymbol{\Sigma}_{c0}^{-1}. \quad \text{(B.5)}$$

Performing the inversion operation on both sides of the above equation, we get

$$\boldsymbol{\Sigma}_c - \boldsymbol{\Sigma}_{c0} = -\left(\boldsymbol{\Sigma}_{c0}^{-1}(\Theta_0^T\boldsymbol{\Sigma}_e^{-1}\Theta_0 + \Theta'^T_0\,\boldsymbol{\Sigma}'^{-1}_e\,\Theta'_0)^{-1}\boldsymbol{\Sigma}_{c0}^{-1} + \boldsymbol{\Sigma}_{c0}^{-1}\right)^{-1}. \quad \text{(B.6)}$$

If we do not consider the covariance of OD demand, it implies that all of the OD pairs are considered as independent, we regard $\boldsymbol{\Sigma}_{c0} = Diag(\boldsymbol{\Sigma}_{c0})$ and $\boldsymbol{\Sigma}_c = Diag(\boldsymbol{\Sigma}_c)$.

Then, $tr(\boldsymbol{\Sigma}_c - \boldsymbol{\Sigma}_{c0}) = -\Bigg(Diag(\boldsymbol{\Sigma}_{c0}^{-1})\left(\Theta_0^T\boldsymbol{\Sigma}_e^{-1}\Theta_0 + \Theta'^T_0\,\boldsymbol{\Sigma}'^{-1}_e\,\Theta'_0\right)^{-1}Diag(\boldsymbol{\Sigma}_{c0}^{-1}) + Diag(\boldsymbol{\Sigma}_{c0}^{-1})\Bigg)^{-1}$.

If we only consider the covariance of OD demand in a single period, then the OD demands in period h_1 should be independent of those in period h_2. Given that there are *k* periods of interest, thus we can regard $\boldsymbol{\Sigma}_{c0} = BDiag(\boldsymbol{\Sigma}_{c0}, k)$ and $\boldsymbol{\Sigma}_c = BDiag(\boldsymbol{\Sigma}_c, k)$. Then,

$tr(\boldsymbol{\Sigma}_c - \boldsymbol{\Sigma}_{c0}) = -\Bigg(BDiag(\boldsymbol{\Sigma}_{c0}^{-1}, k)\left(\Theta_0^T\boldsymbol{\Sigma}_e^{-1}\Theta_0 + \Theta'^T_0\,\boldsymbol{\Sigma}'^{-1}_e\,\Theta'_0\right)^{-1}BDiag(\boldsymbol{\Sigma}_{c0}^{-1}, k) + BDiag(\boldsymbol{\Sigma}_{c0}^{-1}, k)\Bigg)^{-1}$.

As $\boldsymbol{\Sigma}_e$ and $\boldsymbol{\Sigma}'_e$ are both positive definite, the inversion of these two matrices gives $\boldsymbol{\Sigma}_e^{-1}$ and $\boldsymbol{\Sigma}'^{-1}_e$, which are also positive definite, so that all of the elements in the matrix $\Theta_0^T\boldsymbol{\Sigma}_e^{-1}\Theta_0 + \Theta'^T_0\,\boldsymbol{\Sigma}'^{-1}_e\,\Theta'_0$ are positive.

Therefore,

$$\begin{aligned}&\boldsymbol{\Sigma}_{c0}^{-1}(\Theta_0^T\boldsymbol{\Sigma}_e^{-1}\Theta_0 + \Theta'^T_0\,\boldsymbol{\Sigma}'^{-1}_e\,\Theta'_0)^{-1}\boldsymbol{\Sigma}_{c0}^{-1}\\ &\geq BDiag(\boldsymbol{\Sigma}_{c0}^{-1}, k)(\Theta_0^T\boldsymbol{\Sigma}_e^{-1}\Theta_0 + \Theta'^T_0\,\boldsymbol{\Sigma}'^{-1}_e\,\Theta'_0)^{-1}BDiag(\boldsymbol{\Sigma}_{c0}^{-1}, k).\\ &\geq Diag(\boldsymbol{\Sigma}_{c0}^{-1})(\Theta_0^T\boldsymbol{\Sigma}_e^{-1}\Theta_0 + \Theta'^T_0\,\boldsymbol{\Sigma}'^{-1}_e\,\Theta'_0)^{-1}Diag(\boldsymbol{\Sigma}_{c0}^{-1})\end{aligned} \quad \text{(B.7)}$$

Thus, if the traffic sensor locations are given, we can get

$$tr(\boldsymbol{\Sigma}_c - \boldsymbol{\Sigma}_{c0})_{m\text{cov}} \geq tr(\boldsymbol{\Sigma}_c - \boldsymbol{\Sigma}_{c0})_{b\text{cov}} \geq tr(\boldsymbol{\Sigma}_c - \boldsymbol{\Sigma}_{c0})_{no\text{cov}}. \quad \text{(B.8)}$$

The proof is completed.

Appendix C

Proof of Proposition 2

Mathematically, assume that the unit costs of AVI sensors and point sensors have the following relationship: $\beta' = \alpha \cdot \beta$. Denote $[\alpha]$ as a floor function that gives the greatest integer less than or equal to α.

Case 1: If $\left(\Theta'_{rw(h)}\right)^2\left(\varepsilon'_{r(h)}\right)^{-1} > \max\sum_{a=1}^{[\alpha]}\left(\left(\Theta_{aw(h)}\right)^2\left(\varepsilon_{a(h)}\right)^{-1}\right)$ for $\forall r \in \mathbf{R}, a \in \mathbf{A}$, only AVI

sensors should be chosen for the multi-period OD demand estimation.

Case 2: Conversely, if $\left(\Theta'_{rw(h)}\right)^2\left(\varepsilon'_{r(h)}\right)^{-1} < \min\sum_{a=1}^{[\alpha]}\left(\left(\Theta_{aw(h)}\right)^2\left(\varepsilon_{a(h)}\right)^{-1}\right)$ for $\forall r \in \mathbf{R}, a \in \mathbf{A}$, only point sensors should be chosen.

Case 3: However, if $\exists r \in \mathbf{R}, a \in \mathbf{A}$ so that $\min\sum_{a=1}^{[\alpha]}\left(\left(\Theta_{aw(h)}\right)^2\left(\varepsilon_{a(h)}\right)^{-1}\right) \le \left(\Theta'_{rw(h)}\right)^2\left(\varepsilon'_{r(h)}\right)^{-1} \le \max\sum_{a=1}^{[\alpha]}\left(\left(\Theta_{aw(h)}\right)^2\left(\varepsilon_{a(h)}\right)^{-1}\right)$, both AVI and point sensors are needed.

First, we prove Case 1. As shown in Eq. (22a), the objective of multi-type traffic sensor location problem is restated as:

$$\min_{z,z'}\sum_{w\in\mathbf{W},h\in\mathbf{H}}\left(\sum_{w'\in\mathbf{W},h'\in\mathbf{H}}|\sigma_{w(h),w'(h')}|\right)\sigma_{w(h)} \quad . \tag{C.1}$$

For a clear presentation, we denote $\kappa_{w(h)} = \sum_{w'\in\mathbf{W},h'\in\mathbf{H}}|\sigma_{w(h),w'(h')}|$, so that the above equation then becomes

$$\begin{aligned}&\min_{z,z'}\sum_{w\in\mathbf{W},h\in\mathbf{H}}\kappa_{w(h)}\sigma_{w(h)}\\ &\Rightarrow\min_{z,z'}\sum_{w\in\mathbf{W},h\in\mathbf{H}}\kappa_{w(h)}\left(\sigma_{w(h)0}{}^{-1}+\sum_{a\in\mathbf{A}}(\Theta_{aw0(h)})^2(\varepsilon_{a(h)})^{-1}+\sum_{r\in\mathbf{R}}(\Theta'_{rw0(h)})^2(\varepsilon'_{r(h)})^{-1}\right)^{-1}.\end{aligned} \tag{C.2}$$

For Case 1, if $\left(\Theta'_{rw(h)}\right)^2\left(\varepsilon'_{r(h)}\right)^{-1} > \max\sum_{a=1}^{[\alpha]}\left(\left(\Theta_{aw0(h)}\right)^2\left(\varepsilon_{a(h)}\right)^{-1}\right)$ for $\forall r \in \mathbf{R}, a \in \mathbf{A}$, given the fixed budget constraint $\beta\sum z + \beta'\sum z' \le B$ and $\beta' = \alpha\cdot\beta$, it is always satisfied that $\left(\Theta'_{rw(h)}\right)^2\left(\varepsilon'_{r(h)}\right)^{-1} < \left(\max\sum_{a=1}^{[\alpha]}\left(\left(\Theta_{aw0(h)}\right)^2\left(\varepsilon_{a0(h)}\right)^{-1}\right)\right)^{-1}$ for $\forall r \in \mathbf{R}, a \in \mathbf{A}$.

As $\kappa_{w(h)} \ge 0$, the above equation implies that

$$\begin{aligned}&\min_{z,z'}\sum_{w\in\mathbf{W},h\in\mathbf{H}}\kappa_{w(h)}\left(\sigma_{w(h)0}{}^{-1}+\sum_{r\in\mathbf{R}}(\Theta'_{rw0(h)})^2(\varepsilon'_{r(h)})^{-1}\right)^{-1}\\ &\le\min_{z,z'}\sum_{w\in\mathbf{W},h\in\mathbf{H}}\kappa_{w(h)}\left(\sigma_{w(h)0}{}^{-1}+\sum_{a\in\mathbf{A}}(\Theta_{aw0(h)})^2(\varepsilon_{a(h)})^{-1}+\sum_{r\in\mathbf{R}}(\Theta'_{rw0(h)})^2(\varepsilon'_{r(h)})^{-1}\right)^{-1},\end{aligned} \tag{C.3}$$

s. t.

$$\beta\sum z + \beta'\sum z' \le B \quad . \tag{C.4}$$

The proof of Case 1 is completed. Cases 2 and 3 can be easily proved in a similar way.

Appendix D

Sets

A set of links in the road network

W set of OD pairs in the road network

R set of paths or path segments defined by AVI sensors in the road network

H set of periods of interest

D set of days of interest

Size of sets

m number of links in the road network

n number of OD pairs in the road network

k number of periods of interest

Subscripts

h, h' subscript for traffic flow representing the period, $h, h' \in \mathbf{H}$

a, a' subscript for link flow, $a, a' \in \mathbf{A}$

w, w' subscript for OD demand, $w, w' \in \mathbf{W}$

r, r' subscript for path or path segment, $r, r' \in \mathbf{R}$

d subscript for traffic flow representing the date in a year

Vectors and matrices

$\mathbf{v}_{a(h)}$ vector of mean link flows observed by point sensors in period *h*

$\mathbf{v}'_{a(h)}$ vector of mean partial link flows observed by AVI sensors in period *h*

$\mathbf{v}'_{r(h)}$ vector of mean partial path flow observed by AVI sensors in period *h*

$\mathbf{q}_{(h)}$ vector of estimated OD demands in period *h*

$\mathbf{q}_0$ vector of prior OD demands in all periods

$\mathbf{c}$ vector of estimated principal OD demand components in multiple periods

$\mathbf{c}_0$ vector of prior principal OD demand components in multiple periods

$\mathbf{P}_{0(h)}$ matrix of prior link choice proportion in period *h*

$\mathbf{P'}_{0(h)}$ matrix of prior path or path segment choice proportion in period *h*

$\mathbf{P}_{(h)}$ matrix of updated link choice proportion in period *h*

$\mathbf{P'}_{(h)}$ matrix of updated path or path segment choice proportion in period *h*

$\mathbf{P}$ block diagonal matrix of link choice proportion in multiple periods, $\mathbf{P} = \begin{bmatrix} \mathbf{P}_{(h)} & \mathbf{0} \\ \mathbf{0} & \mathbf{P}_{(h')} \end{bmatrix}$

$\mathbf{\Theta}_0$ transformed prior link choice proportion matrix in multiple periods, that is, the transform of the original link choice proportions to the orthonormal basis matrix of eigenvectors $\mathbf{E}$ for OD demand covariance matrix

$\mathbf{\Theta'}_0$ transformed prior path or path segment choice proportion matrix in multiple periods, that is, the transform of the original path or path segment choice proportions to the orthonormal basis matrix of eigenvectors $\mathbf{E}$ for OD demand covariance matrix

$\mathbf{\Theta}_{(h)}$ transformed updated link choice proportion matrix

$\mathbf{\Theta'}_{(h)}$ transformed updated path or path segment choice proportion matrix

$\mathbf{\Sigma}_v$ covariance matrix of link flow observed by point sensors in multiple periods

$\mathbf{\Sigma}_q$ covariance matrix of estimated OD demand in multiple periods

$\mathbf{\Sigma}_{q0}$ covariance matrix of prior OD demand in multiple periods

$\mathbf{\Sigma}_c$ covariance matrix of estimated principal OD demand components in multiple periods

$\mathbf{\Sigma}_{c0}$ covariance matrix of prior principal OD demand components in multiple periods

$\mathbf{\Sigma}_e$ covariance matrix of measurement error from point sensors

$\mathbf{\Sigma'}_e$ covariance matrix of measurement error from AVI sensors

$\mathbf{K}$ updating gain matrix for observations from point sensors, also refer to as Kalman gain

$\mathbf{K'}$ updating gain matrix for observations from AVI sensors

Variables

Decision variables

z point sensor locations

z' AVI sensor locations

$q_{w(h)}$ traffic demand in OD pair *w* during period *h*

$\sigma_{w(h),w'(h')}$ covariance estimate of traffic demands between OD pairs *w* in period h and w' in period h'

Observations

$v_{a(h)}$ mean of hourly traffic flow on link *a* observed by point sensors in period *h*

$v'_{a(h)}$ mean of partial traffic flow on link *a* observed by AVI sensors in period *h*

$v'_{r(h)}$ mean of partial traffic flow on path or path segment *r* observed by AVI sensors in period *h*

$\sigma_{v_{a(h)},v_{a'(h')}}$ covariance of point sensor observation between link flows v_a during period h and $v_{a'}$ during period h'

$\sigma_{a'_{r(h)},v'_{a'(h')}}$ covariance of AVI sensor observation between partial link flows v'_a during period h and $v'_{a'}$ during period h'

$\sigma_{v'_{r(h)},v'_{r'(h')}}$ covariance of AVI sensor observation between partial path flows v'_r during period h and $v'_{r'}$ during period h'

Parameters

M number of principal OD demand components

$q_{w(h)0}$ prior OD demand for OD pair w during period h

$\sigma_{w(h),w'(h')0}$ covariance of prior OD demand between OD pairs w in period h and w' in period h'

$p_{aw(h)}$ link choice proportion of OD pair *w* passing through link *a* in period *h*

$p'_{rw(h)}$ path or path segment choice proportion, that is, the proportion of traffic demand in OD pair w passing through path or path segment r in period h

π_a penetration rate for tagged vehicles on link *a*

π average penetration rate for tagged vehicles on all links

ε_a measurement error of traffic flow on link a observed by point sensor(s)

ε'_r measurement error of traffic flow on link, path, or path segment r observed the AVI sensor(s)

β installation and maintenance cost for a point sensor

β' installation and maintenance cost for an AVI sensor

B total budget for the sensor installation

References

Antoniou, C., Ben-Akiva, M., Koutsopoulos, H.N., 2004. Incorporating automated vehicle identification data into origin-destination estimation. Transportation Research Record: Journal of the Transportation Research 1882, 37–44.

Ashok, K., Ben-Akiva, M.E., 1993. Dynamic origin-destination matrix estimation and prediction for real-time traffic management systems, in: Daganzo, C. (Ed.), Proceedings of the 12th International Symposium on Transportation. Elsevier, pp. 465–484.

Ballis, H., Dimitriou, L., 2020. Revealing personal activities schedules from synthesizing multi-period

origin-destination matrices. Transportation Research Part B: Methodological 139, 224–258.

Bhat, C.R., Goulias, K.G., Pendyala, R.M., Paleti, R., Sidharthan, R., Schmitt, L., Hu, H.H., 2013. A household-level activity pattern generation model with an application for Southern California. Transportation 40, 1063–1086.

Bianco, L., Confessore, G., Reverberi, P., 2001. A network based model for traffic sensor location with implications on O/D matrix estimates. Transportation Science 35, 50–60.

Bierlaire, M., 2002. The total demand scale: a new measure of quality for static and dynamic origin–destination trip tables. Transportation Research Part B: Methodological 36, 837–850.

Caggiani, L., Ottomanelli, M., Sassanelli, D., 2013. A fixed point approach to origin-destination matrices estimation using uncertain data and fuzzy programming on congested networks. Transportation Research Part C: Emerging Technologies 28, 130–141.

Cantelmo, G., Qurashi, M., Prakash, A.A., Antoniou, C., Viti, F., 2020. Incorporating trip chaining within online demand estimation. Transportation Research Part B: Methodological 132, 171–187.

Cascetta, E., 2009. Transportation systems analysis: models and applications, Springer Science & Business Media.

Cascetta, E., Nguyen, S., 1988. A unified framework for estimating or updating origin/destination matrices from traffic counts. Transportation Research Part B: Methodological 22, 437–455.

Castillo, E., Gallego, I., Menéndez, J.M., Jiménez, P., 2011. Link flow estimation in traffic networks on the basis of link flow observations. Journal of Intelligent Transportation Systems 15, 205–222.

Castillo, E., Menéndez, J.M., Sánchez-Cambronero, S., 2008. Traffic estimation and optimal counting location without path enumeration using bayesian networks. Computer-Aided Civil and Infrastructure Engineering 23, 189–207.

Chootinan, P., Chen, A., 2011. Confidence interval estimation for path flow estimator. Transportation Research Part B: Methodological 45, 1680–1698.

Djukic, T., Flötteröd, G., Van Lint, H., Hoogendoorn, S., 2012. Efficient real time OD matrix estimation based on Principal Component Analysis, in: IEEE Conference on Intelligent Transportation Systems, Proceedings, ITSC. pp. 115–121.

Fei, X., Mahmassani, H.S., Murray-Tuite, P., 2013. Vehicular network sensor placement optimization under uncertainty. Transportation Research Part C: Emerging Technologies 29, 14–31.

Fu, C., Zhu, N., Ling, S., Ma, S., Huang, Y., 2016. Heterogeneous sensor location model for path reconstruction. Transportation Research Part B: Methodological 91, 77–97.

Fu, C., Zhu, N., Ma, S., 2017. A stochastic program approach for path reconstruction oriented sensor location model. Transportation Research Part B: Methodological 102, 210–237.

Fu, H., Lam, W.H.K., Shao, H., Xu, X.P., Lo, H.P., Chen, B.Y., Sze, N.N., Sumalee, A., 2019. Optimization of traffic count locations for estimation of travel demands with covariance between origin-destination flows. Transportation Research Part C: Emerging Technologies 108, 49–73.

Gentili, M., Mirchandani, P.B., 2018. Review of optimal sensor location models for travel time estimation. Transportation Research Part C: Emerging Technologies 90, 74–96.

Gentili, M., Mirchandani, P.B., 2012. Locating sensors on traffic networks: models, challenges and research opportunities. Transportation Research Part C: Emerging Technologies 24, 227–255.

Goel, P., Kulik, L., Ramamohanarao, K., 2016. Optimal pick up point selection for effective ride sharing. IEEE Transactions on Big Data 3, 154–168.

Gu, Y., Fu, X., Liu, Z., Xu, X., Chen, A., 2020. Performance of transportation network under perturbations: Reliability, vulnerability, and resilience. Transportation Research Part E: Logistics

and Transportation Review 133, 101809.

Hu, S.R., Peeta, S., Liou, H.T., 2016. Integrated determination of network origin-destination trip matrix and heterogeneous sensor selection and location strategy. IEEE Transactions on Intelligent Transportation Systems 17, 195–205.

Huang, H.J., 2002. Pricing and logit-based mode choice models of a transit and highway system with elastic demand. European Journal of Operational Research 140, 562–570.

Jati, G.K., Suyanto, 2011. Evolutionary discrete firefly algorithm for travelling salesman problem. Adaptive and Intelligent Systems. ICAIS 2011. 393–403.

Jolliffe, I.T., 2002. Principal component analysis. Springer, New York, US.

Jones, L.K., Gartner, N.H., Shubov, M., Stamatiadis, C., Einstein, D., 2018. Modeling origin-destination uncertainty using network sensor and survey data and new approaches to robust control. Transportation Research Part C: Emerging Technologies 94, 121–132.

Krishnakumari, P., van Lint, H., Djukic, T., Cats, O., 2020. A data driven method for OD matrix estimation. Transportation Research Part C: Emerging Technologies 113, 38–56.

Lam, W.H.K., Xu, G., 1999. A traffic flow simulator for network reliability assessment. Journal of Advanced Transportation 33, 159–182.

Li, Z., 2018. Unobserved and observed heterogeneity in risk attitudes: Implications for valuing travel time savings and travel time variability. Transportation Research Part E: Logistics and Transportation Review 112, 12–18.

Liu, P., Liu, J., Ong, G.P., Tian, Q., 2020. Flow pattern and optimal capacity in a bi-modal traffic corridor with heterogeneous users. Transportation Research Part E: Logistics and Transportation Review 133, 101831.

Liu, Z., Meng, Q., Wang, S., Sun, Z., 2014. Global intermodal liner shipping network design. Transportation Research Part E: Logistics and Transportation Review 61, 28–39.

Lo, H.P., Zhang, N., Lam, W.H.K., 1996. Estimation of an origin-destination matrix with random link choice proportions: a statistical approach. Transportation Research Part B: Methodological 30, 309–324.

Maher, M.J., 1983. Inferences on trip matrices from observations on link volumes: a Bayesian statistical approach. Transportation Research Part B: Methodological 17, 435–447.

Marzano, V., Papola, A., Simonelli, F., Papageorgiou, M., 2018. A Kalman filter for quasi-dynamic o-d flow estimation/updating. IEEE Transactions on Intelligent Transportation Systems 19, 3604–3612.

Meng, Q., Hei, X., Wang, S., Mao, H., 2015a. Carrying capacity procurement of rail and shipping services for automobile delivery with uncertain demand. Transportation Research Part E: Logistics and Transportation Review 82, 38–54.

Meng, Q., Wang, T., 2011. A scenario-based dynamic programming model for multi-period liner ship fleet planning. Transportation Research Part E: Logistics and Transportation Review 47, 401–413.

Meng, Q., Wang, T., Wang, S., 2015b. Multi-period liner ship fleet planning with dependent uncertain container shipment demand. Maritime Policy & Management 42, 43–67.

Meng, Q., Zhao, H., Wang, Y., 2019. Revenue management for container liner shipping services: Critical review and future research directions. Transportation Research Part E: Logistics and Transportation Review 128, 280–292.

Mirchandani, P.B., Gentili, M., He, Y., 2009. Location of vehicle identification sensors to monitor travel-time performance. IET Intelligent Transport Systems 3, 289–303.

Nayeem, M.A., Rahman, M.K., Rahman, M.S., 2014. Transit network design by genetic algorithm with

elitism. Transportation Research Part C: Emerging Technologies 46, 30–45.

Ohazulike, A.E., Still, G., Kern, W., van Berkum, E.C., 2013. An origin-destination based road pricing model for static and multi-period traffic assignment problems. Transportation Research Part E: Logistics and Transportation Review 58, 1–27.

Pal, S.K., Rai, C.S., Singh, A.P., 2012. Comparative study of firefly algorithm and particle swarm optimization for noisy non-linear optimization problems. Intelligent Systems and Applications 10, 50–57.

Park, H., Haghani, A., 2015. Optimal number and location of Bluetooth sensors considering stochastic travel time prediction. Transportation Research Part C: Emerging Technologies 55, 203–216.

Parry, K., Hazelton, M.L., 2012. Estimation of origin-destination matrices from link counts and sporadic routing data. Transportation Research Part B: Methodological 46, 175–188.

Salari, M., Kattan, L., Lam, W.H.K., Lo, H.P., Esfeh, M.A., 2019. Optimization of traffic sensor location for complete link flow observability in traffic network considering sensor failure. Transportation Research Part B: Methodological 121, 216–251.

Sayadi, M.K., Ramezanian, R., Ghaffari-Nasab, N., 2010. A discrete firefly meta-heuristic with local search for makespan minimization in permutation flow shop scheduling problems. International Journal of Industrial Engineering Computations 1, 1–10.

Shao, H., Lam, W.H.K., Sumalee, A., Chen, A., Hazelton, M.L., 2014. Estimation of mean and covariance of peak hour origin–destination demands from day-to-day traffic counts. Transportation Research Part B: Methodological 68, 52–75.

Shao, H., Lam, W.H.K., Sumalee, A., Hazelton, M.L., 2015. Estimation of mean and covariance of stochastic multi-class OD demands from classified traffic counts. Transportation Research Part C: Emerging Technologies 7, 192–211.

Simonelli, F., Marzano, V., Papola, A., Vitiello, I., 2012. A network sensor location procedure accounting for o–d matrix estimate variability. Transportation Research Part B: Methodological 46, 1624–1638.

Siripirote, T., Sumalee, A., Ho, H.W., 2020. Statistical estimation of freight activity analytics from Global Positioning System data of trucks. Transportation Research Part E: Logistics and Transportation Review 140, 101986.

Sun, W., Shao, H., Shen, L., Wu, T., Lam, W.H.K., Yao, B., Yu, B., 2021. Bi-objective traffic count location model for mean and covariance of origin–destination estimation. Expert Systems with Applications 170, 114554.

Transport Department, 2021. Speed Map Panels, Transport Department, Government of the Hong Kong SAR.

Transport Department, 2018. The Annual Traffic Census 2017, Traffic and Transport Survey Division, Transport Department, Government of the Hong Kong SAR.

Transport Department, 2004. The 2004 Base District Traffic Models, Transport Planning Division, Transport Department, Government of the Hong Kong SAR.

Van Zuylen, H.J., Willumsen, L.G., 1980. The most likely trip matrix estimated from traffic counts. Transportation Research Part B: Methodological 14, 281–293.

Wang, H., Meng, Q., Zhang, X., 2020. Multiple equilibrium behaviors of auto travellers and a freight carrier under the cordon-based large-truck restriction regulation. Transportation Research Part E: Logistics and Transportation Review 134, 101829.

Wang, H., Zhang, X., 2016. Joint implementation of tradable credit and road pricing in public-private partnership networks considering mixed equilibrium behaviors. Transportation Research Part E:

Logistics and Transportation Review 94, 158–170.

Xing, T., Zhou, X., Taylor, J., 2013. Designing heterogeneous sensor networks for estimating and predicting path travel time dynamics: An information-theoretic modeling approach. Transportation Research Part B: Methodological 57, 66–90.

Xiong, T., Bao, Y., Hu, Z., 2014. Multiple-output support vector regression with a firefly algorithm for interval-valued stock price index forecasting. Knowledge-Based Systems 55, 87–100.

Xu, X., Lo, H.K., Chen, A., Castillo, E., 2016. Robust network sensor location for complete link flow observability under uncertainty. Transportation Research Part B: Methodological 88, 1–20.

Yang, H., Iida, Y., Sasaki, T., 1991. An analysis of the reliability of an origin-destination trip matrix estimated from traffic counts. Transportation Research Part B: Methodological 25, 351–363.

Yang, H., Sasaki, T., Iida, Y., 1992. Estimation of origin-destination matrices from link traffic counts on congested networks. Transportation Research Part B: Methodological 26, 417–434.

Yang, H., Zhou, J., 1998. Optimal traffic counting locations for origin–destination matrix estimation. Transportation Research Part B: Methodological 32, 109–126.

Yang, X.-S., 2008. Firefly algorithm, in: Nature-Inspired Metaheuristic Algorithms. Luniver Press, London, UK.

Yin, B., Liu, L., Coulombel, N., Viguié, V., 2017. Evaluation of ridesharing impacts using an integrated transport land-use model: A case study for the Paris region, in: Transportation Research Procedia. Elsevier B.V., pp. 824–831.

Yu, Q., Zhu, N., Li, G., Ma, S., 2015. Simulation-based sensor location model for arterial street. Discrete Dynamics in Nature and Society 2015, 1–13.

Zhou, X., List, G.F., 2010. An information-theoretic sensor location model for traffic origin-destination demand estimation applications. Transportation Science 44, 254–273.

Zhu, N., Fu, C., Ma, S., 2018. Data-driven distributionally robust optimization approach for reliable travel-time-information-gain-oriented traffic sensor location model. Transportation Research Part B: Methodological 113, 91–120.

Zhu, N., Liu, Y., Ma, S., He, Z., 2014. Mobile traffic sensor routing in dynamic transportation systems. IEEE Transactions on Intelligent Transportation Systems 15, 2273–2285.

Zhu, Y., He, Z., Sun, W., 2019. Network-wide link travel time inference using trip-based data from automatic vehicle identification detectors. IEEE Transactions on Intelligent Transportation Systems 21, 1–11.